10
Kinetics of Homogeneous Hydrogenations: Measurement and Interpretation

Hans-Joachim Drexler, Angelika Preetz, Thomas Schmidt, and Detlef Heller

10.1
Introduction

Recently, the results of kinetic measurements have been summarized for homogeneous hydrogenations with transition metal complexes in a review [1]. Essential new results of kinetic investigations leading to the completion of hitherto existing ideas regarding the reaction mechanism of particular catalyses are represented in the respective chapters of this book, and shall not be repeated here. Rather, this chapter will introduce the kinetic treatment of reaction sequences with pre-equilibria typical for catalyses, together with the analysis and interpretation of Michaelis-Menten kinetics, the monitoring of hydrogenations, and a discussion of possible problems, with selected examples.

Kinetic investigations deliver quantitative correlations regarding the concentration–time dependence of the participating reactants, and therefore serve as the major methodical approach in the elucidation of reaction mechanisms. A knowledge of funded mechanistic ideas opens the possibility of an aimed manipulation of activity and selectivity, respectively, which are important parameters of catalyses. As "operating values", pressure and temperature – as well as the concentration of particular reaction partners – are available. However, when scaling-up from a laboratory standard to an industrial application, kinetic results are indispensable. Moreover, kinetics provides essential indications about the nature of the actual catalyst and the distinction between homogeneous and heterogeneous catalysis. This objective has been investigated more intensively during the past few years, partly with surprising results, and naturally plays an important role when transition-metal complexes meet with hydrogen as reducing agent [2]. Thereby, the problem does not lie in the kinetics as the method. ("In the kinetic approach no frontiers exist today between homogeneous, enzymatic, and heterogeneous catalysis. There is a consistent science which permits the definition of useful and efficient rate laws describing sequences of elementary steps." [3])

In spite of these capabilities of kinetics it is necessary to emphasize here that, in principle, it is not possible to *prove* that a reaction mechanism occurs only by

The Handbook of Homogeneous Hydrogenation.
Edited by J. G. de Vries and C. J. Elsevier

ISBN: 978-3-527-31161-3

using kinetic investigations! Rather, it is the nature of kinetics to describe quantitative dependences between reaction partners and thus to exclude specific reaction sequences. This model discrimination, however, does not principally allow the favoring of one reaction mechanism among a few remaining possibilities [4]. Furthermore, it is possible that formal-kinetically equivalent reaction sequences are chemically different and hence are not to be distinguished by merely applying kinetic methods [5]. Only additional findings such as the detection (or rather the isolation) of intermediates, the interpretation of isotope labeling studies, as well as computational chemistry, allow descriptions to be made of experimental results which are consistent in the form of a closed catalytic cycle – the reaction mechanism most probable on the basis of the existing indications.

There is, however, no doubt about the significance of kinetics for catalysis as the following statements indicate:

- "Kinetic measurements are essential for the elucidation of any catalytic mechanism since catalysis, by definition and significance, is purely a kinetic phenomenon" [6].
- "Asymmetric catalysis is four-dimensional chemistry. Simple stereochemical scrutiny of the substrate or reagent is not enough. The high efficiency that the reactions provide can only be achieved through a combination of both an ideal three-dimensional structure (x,y,z) and suitable kinetics (t)" [7].
- "Carefully determined conversion–time diagrams, *in-situ* spectroscopic studies and, if possible, kinetic time laws belong to the fundamentals of catalysis research and are prerequisites for a mechanistic understanding" [8].

Although the outstanding relevance of kinetics is clear, very few publications relate to in-depth kinetic analyses. The reasons for this are complex, and some of these are detailed below:

- The field of homogeneous catalysis deals primarily with the organometallic complex catalysis, besides organocatalysis, which is at present experiencing a renaissance [9]. One problem of most of the transition-metal complexes used today is a need for anaerobic reaction conditions, and this is why many conventional possibilities of kinetic investigations are restricted in their application.
- A further problem results from the catalysis itself. Only the permanent repetition of a catalytic cycle demonstrates clearly the advantage of catalysis over a simple stoichiometric reaction. A good catalyst must be very effective, leading to a desired product with a high turnover number (TON, defined as moles of substrate per mole of catalyst) and turnover frequency (TOF, defined as TON per unit time) [10–12]. Because of the large substrate : catalyst ratio, however, detailed kinetic investigations are complicated as the interesting intermediates of the catalytic cycle must be detected and quantified, beside large quantities of substrate and/or product. In addition, in a catalytic cycle, the amount of transition-metal complex is shared by several intermediates. In the case of stereoselective catalyses, the number of relevant intermediates might also easily be multiplied [13]. Furthermore, one condition of catalytic reaction se-

quences with transition-metal complexes must not be neglected, namely that intermediates can relatively easily be transposed into one another, mostly reversibly. Due to disadvantageous equilibrium positions, the intermediates might not be detectable, even under stationary catalytic conditions [14].

- In almost every case differential equations for the quantitative description of the time dependence of particular species resulting from a catalytic cycle cannot be solved directly. This requires approximate solutions to be made, such as the equilibrium approximation [15], the Bodenstein principle [16], or the more generally valid steady-state approach [17]. A discussion of differences and similarities of different approximations can be found in [18].
- Another problem arises from the fact that good kinetic studies in the field of homogeneous catalysis require not only complex-chemical and methodical experience, but also a solid knowledge of physical chemistry. Yet, this additional requirement is seldom requested at a time when financial pressure on research is steadily growing [19].

10.2
The Basics of Michaelis-Menten Kinetics

Most catalytic cycles are characterized by the fact that, prior to the rate-determining step [18], intermediates are coupled by equilibria in the catalytic cycle. For that reason Michaelis-Menten kinetics, which originally were published in the field of enzyme catalysis at the start of the last century, are of fundamental importance for homogeneous catalysis. As shown in the reaction sequence of Scheme 10.1, the active catalyst first reacts with the substrate in a pre-equilibrium to give the catalyst–substrate complex [20]. In the rate-determining step, this complex finally reacts to form the product, releasing the catalyst.

Under isobaric conditions ($k_2 = k_2' \cdot [H_2]$), many hydrogenations exactly follow this model. The classical example is the asymmetric hydrogenation of prochiral dehydroamino acid derivatives with Rh or Ru catalysts [21].

The so-called Michaelis-Menten equation (Eq. 1) [22] follows independently of the approximation chosen to solve the differential equation resulting from Scheme 10.1. Its derivation in detail can, for example, be found in [23].

$$V = \frac{dP}{dt} = \frac{k_2 \cdot [E]_0 \cdot [S]}{K_M + [S]} = \frac{V_{sat} \cdot [S]}{K_M + [S]} \tag{1}$$

with (a) $K_M = \frac{k_{-1}}{k_1} = \frac{[E] \cdot [S]}{[ES]}$, (b) $K_M = \frac{k_{-1} + k_2}{k_1} = \frac{[E] \cdot [S]}{[ES]}$,

(c) $K_M = \frac{k_2}{k_1} = \frac{[E] \cdot [S]}{[ES]}$

where (a) is the equilibrium approximation; (b) is the steady-state approach; and (c) is the irreversible formation of the substrate complex ($k_{-1}=0$).

$$E + S \underset{k_{-1}}{\overset{k_1}{\rightleftharpoons}} ES \xrightarrow{k_2} P + (E)$$

Scheme 10.1 Reaction sequence of the simplest case of Michaelis-Menten kinetics. E = catalyst; S = substrate; ES = catalyst–substrate complex; P = product; k_i = rate constants.

The Michaelis-Menten equation is characterized by two constants:

- the rate constant for the reaction of the catalyst–substrate complex to the product (k_2); and
- the Michaelis constant (K_M).

A more detailed examination shows that, in case of equilibrium approximation, the value of K_M corresponds to the inverse stability constant of the catalyst–substrate complex, whereas in the case of the steady-state approach the rate constant of the (irreversible) product formation is additionally included. As one cannot at first decide whether or not the equilibrium approximation is reasonable for a concrete system, care should be taken in interpreting K_M-values as inverse stability constants. At best, the reciprocal of K_M represents a lower limit of a "stability constant"! In other words, the stability constant quantifying the pre-equilibrium can never be smaller than the reciprocal of the Michaelis constant, but can well be significantly higher.

The Michaelis constant has the dimension of a concentration and characterizes – independently of the method of approximation – the substrate concentration at which the ratio of free catalyst to catalyst–substrate complex equals unity. At this point, exactly one-half of the catalyst is complexed by the substrate. Likewise, one finds that at a value of $[S] = 10\ K_M$, the ratio of [E]/[ES]

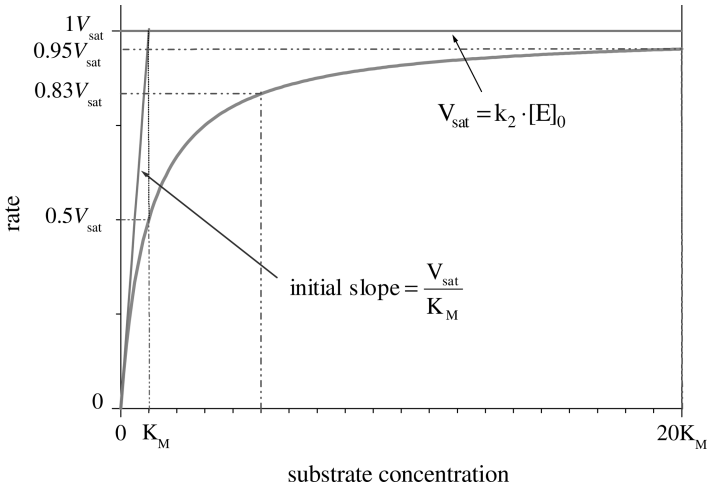

Fig. 10.1 Product formation rate as a function of substrate concentration (Eq. (1)).

equals 0.1, which means that virtually 91% of the initial catalyst ($[E_0]$) is present as substrate complex. The product formation rate is shown schematically as a function of substrate concentration in Figure 10.1.

Because of the complexity of biological systems, Eq. (1) as the differential form of Michaelis-Menten kinetics is often analyzed using the initial rate method. Due to the restriction of the initial range of conversion, unwanted influences such as reversible product formation, effects due to enzyme inhibition, or side reactions are reduced to a minimum. The major disadvantage of this procedure is that a relatively large number of experiments must be conducted in order to determine the desired rate constants.

An analysis of the product formation is, in principle, not limited to the initial range of rates, however. Laidler investigated the problem of the validity range of the Michaelis-Menten equation as a function of time under the assumption of steady-state conditions for the catalyst–substrate complex [24]. As long as either condition shown in Eq. (2) is fulfilled – by choice of experimental conditions it is usually $[S]_0 >> [E]_0$ – Eq. (3) applies up to high conversions for hydrogenations, which corresponds to Eq. (1) [23]. In fact, each point of a hydrogenation curve can be understood as an "initial rate experiment". By analyzing a hydrogenation over a wide range of conversion, a large number of initial rate experiments can be omitted. "Reaction progress kinetic analysis" as a powerful methodology was very recently described by Blackmond in a highly recommended review [25].

$$[S]_0 \gg [E]_0 \;\; [E]_0 \gg [S]_0 \;\; k_{-1} + k_2 \gg k_1 \cdot [E]_0 \;\; k_{-1} + k_2 \gg k_1 \cdot [S]_0 \tag{2}$$

$$\frac{d[P]}{dt} = \frac{k_2 \cdot [E]_0 \cdot ([S]_0 - n_{H_2})}{K_M + ([S]_0 - n_{H_2})} \quad (n_{H_2} = \text{hydrogen consumption}) \tag{3}$$

There are two limiting cases of Michaelis-Menten kinetics. Beginning from Eq. (1) at high substrate excesses (or very small Michaelis constants) Eq. (4a) results. This corresponds to a zero-order reaction with respect to the substrate, the rate of product formation being independent of the substrate concentration. In contrast, very low substrate concentrations [26] (or large Michaelis constants) give the limiting case of first-order reactions with respect to the substrate, Eq. (4b):

$$\text{(a) } V = \frac{d[P]}{dt} = k_2 \cdot [E]_0 = V_{sat} \text{ [27]} \quad \text{(b) } V = \frac{d[P]}{dt} = \frac{k_2 \cdot [E]_0}{K_M} \cdot [S] = k_{obs} \cdot [S] \tag{4}$$

In Figure 10.1, it can be seen that even with substrate excesses of $[S] = 20\ K_M$, the saturation range is not yet reached. Conversely, the data in Figure 10.2 indicate that even for very small substrate concentrations ($[S] = 0.05\ K_M$) the limiting case for the first-order reaction – when the rate is directly proportional to the substrate concentration – is not identical with the values from Eq. (1).

Since methods to analyze Michaelis-Menten kinetics have been sufficiently described in the literature [23, 28], this problem is discussed only briefly at this point.

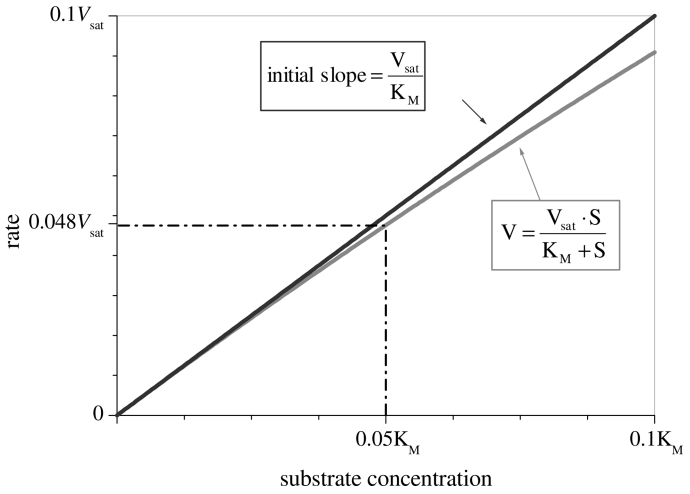

Fig. 10.2 Comparison of Eq. (1) (upper line) with the limiting case of a first-order reaction Eq. (4b) (lower line) for very low substrate concentrations.

In principle, the differential form (Eq. (1)), as well as the integrated form (Eq. (8)), can be used. The differential form of the Michaelis-Menten equation is applied in many cases, since differential values (e.g., flow meter or heat flow data) are often available; by contrast, time-dependent substrate or product concentrations (or proportional quantities) can easily be differentiated numerically.

Initial values for a non-linear fit of Eq. (1) can be achieved by linearizations. Most conventional linearizations result from the transformation of the Michaelis-Menten equation, and are plotted according to:

$$\text{Lineweaver-Burk [29]:} \quad \frac{1}{V} = \frac{K_M}{V_{sat}} \cdot \frac{1}{[S]} + \frac{1}{V_{sat}} \quad \text{plot}: 1/V \text{ versus } 1/[S] \tag{5}$$

$$\text{Eadie-Hofstee [30]:} \quad V = V_{sat} - \frac{V}{[S]} \cdot K_M \quad \text{plot}: V \text{ versus } V/[S] \tag{6}$$

$$\text{Hanes [31]:} \quad \frac{[S]}{V} = \frac{K_M}{V_{sat}} + \frac{1}{V_{sat}} \cdot [S] \quad \text{plot}: [S]/V \text{ versus } [S] \tag{7}$$

An analysis of the influence of errors shows clearly that the double-reciprocal plot according to Lineweaver-Burk [32] is the least suitable. "Although it is by far the most widely used plot in enzyme kinetics, it cannot be recommended, because it gives a grossly misleading impression of the experimental error: for small values of v small errors in v lead to enormous errors in $1/v$, but for large values of v the same small errors in v lead to barely noticeable errors in $1/v$" [23]. Due to the error distribution, that is much more uniform, the plot according to Hanes (Eq. (7)), is the most favored.

The integrated form of the simple Michaelis-Menten kinetics (Eq. (8)), is most suitable to analyze the time-dependent progressive substrate conversion or the corresponding product formation.

$$\frac{1}{t} \cdot \ln \frac{[S]_0}{[S]_t} = -\frac{[P]_t}{K_M \cdot t} + \frac{V_{sat}}{K_M} \tag{8}$$

A more detailed discussion of further possibilities for the analysis of Eq. (1) can be found in [23].

In homogeneous catalysis, the quantification of catalyst activities is commonly carried out by way of TOF or half-life. From a kinetic point of view, the comparison of different catalyst systems is only reasonable if, by giving a TOF, the reaction is zero order or, by giving a half-time, it is a first-order reaction. Only in those cases is the quantification of activity independent of the substrate concentration utilized!

As derived above, there are two limiting cases of Michaelis-Menten kinetics, which is often the basis of homogeneous catalysis. Depending upon the substrate concentration, a reaction of either first or zero order is possible as a limiting case. For hydrogenations of various substrates involving pre-equilibria, reaction orders of unity or zero have been reported for the substrate. Data relating to the kinetics of homogeneous hydrogenations with transition metal complexes before the year 2000 can be found in reference [1], and more recent examples in reference [33] (olefins: [21 c, 33 a–h]; ketones: [33 i–k]; imines: [33 l]; alkynes: [33 m]; nitro groups: [33 m]; N-hetero aromatic compounds: [33 n, o]; CO_2: [33 p]).

If a reaction that must be investigated follows a reaction sequence as in Scheme 10.1, and if the reaction order for the substrate equals unity, it means that (with reference to Eq. (4 b)), the observed rate constant (k_{obs}) is a complex term. Without further information, a conclusion about the single constants k_2 and K_M is not possible. Conversely, from the limiting case of a zero-order reaction, the Michaelis constant cannot be determined for the substrate. For particular questions such as the reliable comparison of activity of various catalytic systems, however, both parameters are necessary. If they are not known, the comparison of catalyst activities for given experimental conditions can produce totally false results. This problem is described in more detail for an example of asymmetric hydrogenation (see below).

10.3
Hydrogenation From a Kinetic Viewpoint

10.3.1
Measurement of Concentration–Time Data and Possible Problems

There exists a multitude of possibilities to monitor hydrogenations in various pressure ranges. In principle, isochoric and isobaric techniques are feasible. In the latter case, the kinetics allows simplification because the concentration of

the reaction partner, hydrogen, is constant. The classical method for measuring concentration–time data is to take samples from the reaction vessel during the hydrogenation, and then to analyze those samples via common methods such as gas chromatography (GC), high-performance liquid chromatography (HPLC), and nuclear magnetic resonance (NMR). In so doing, the sampling over various temperature and pressure ranges can be automated, as can the analysis. The advantage of this method is that any eventually occurring intermediates are detected individually as a function of time, and thus are accessible for kinetic interpretation. The disadvantage, however, is the major analytical effort required. For rapid reactions this method is also hardly appropriate. Moreover, it is sometimes difficult to stop the reaction immediately after sampling, this being a problem which is often underestimated.

A significantly more elegant solution is an *in-situ* monitoring of hydrogenations, as this advantageously provides a large amount of data available for analyses.

Both integrally and differentially measured values can be detected *in situ*. In the first case, substrate- or product-specific signals, or directly proportional quantities, are suitable. Hence, Noyori describes the monitoring of a ketone hydrogenation via the intensity of the infra-red (IR) carbonyl stretching band at 1750 cm^{-1} [21c]. To register the hydrogen consumption of a hydrogenation, a product-proportional concentration as a function of time is monitored. However, the measurement of rates – for example using flow meters or via a heat flow with a calorimeter – represents a typical differential method.

In those cases where concentrations are not measured directly, the problem of "calibration" of the *in-situ* technique becomes apparent. An assurance must be made that no additional effects are registered as systematic errors. Thus, for an isothermal reaction, calorimetry as a tool for kinetic analysis, heat of mixing and/or heat of phase transfer can systematically falsify the measurement. A detailed discussion of the method and possible error sources can be found in [34].

High-throughput methods for catalyst screening and optimization, as described in the literature even for hydrogenations [35], are not suitable for kinetic analyses in most cases.

10.3.1.1 **Monitoring of Hydrogenations via Hydrogen Consumption**

One method, which is still used frequently to follow hydrogenations *in situ*, is the registration of hydrogen consumption. There is a multitude of solutions that can be simply subdivided into normal-pressure and high-pressure measurements. Due to common isobaric reaction conditions the hydrogen concentration is constant, which simplifies kinetics. An isochoric mode of operation is not advisable because of the complexity of the measurement. In fact, the decreasing hydrogen concentration in solution during the course of the hydrogenation must also be taken into account.

For hydrogen, deviations from the ideal gas law must be considered only at higher pressures [36]. Nonetheless, the virial equation allows the amount of hydrogen to be calculated, for example in a reservoir of known volume, by apply-

ing Eq. (9). By using mass balances – based on the initial pressure or cumulatively on the previous value – hydrogen consumption can be determined with accuracy [37]. The problem of such measurements rather lies in a possible temperature gradient between the reservoir and the reaction vessel.

$$n_{H_2} = \frac{\text{reservoir volume}}{\text{real molar volume}} \quad \text{real molar volume} = \frac{R \cdot T}{p} + B + \left(\frac{C - B^2}{R \cdot T}\right) \qquad (9)$$

where R=gas constant, T=temperature, p=pressure, and B and C=virial coefficients.

For flow rate measurements the volume or, more conveniently, the mass flow is suitable. In the first case a pressure- and temperature-dependent calibration is necessary if the gas does not show ideal behavior. This also applies for heat conductivity as the measured quantity often used in flow meters. Currently, real pressure- and temperature-independent measurement of a hydrogen mass flow of a hydrogenation remains problematic on the laboratory scale, at least for low substrate concentrations.

By contrast, the measurement of the hydrogen consumption under normal pressure is relatively simple. The elementary structure of many such measuring devices is similar, and is based principally on the fact that the pressure drop is balanced by reduction in the reaction volume or by supply of the consumed gas, thus ensuring isobaric conditions. An appropriate device for monitoring major gas consumptions is described in [38].

For hydrogenations under normal pressure and isobaric conditions, we use a device which registers gas consumption automatically (Fig. 10.3). Possible error sources resulting from such gas consumption measurements and possibilities of their minimization will be discussed.

The basic principle to realize isobaric conditions for the hydrogenation apparatus shown in Figure 10.3 is to change the volume of the closed reaction space via a (not commercially available) gas-tight syringe in order to ensure a permanent atmospheric pressure as the reference. For this purpose, a sensible pressure sensor registers the pressure drop caused by hydrogen consumption in the closed reaction system. Using a processor-controlled stepping motor axis, the piston of the syringe is depressed until the initial pressure is reached. At this point the position of the piston is registered as a function of time and finally visualized as the hydrogenation curve. (The same arrangement also allows the automatic registration of gas formation.)

This method, although being used analogously in other devices, incorporates a number of principal error sources. These result substantially from transport phenomena, vapor pressure of the solvent, gas solubility, and tempering problems. Particular points, together with possible means of their minimization, will be discussed in the following section.

One problem encountered when monitoring gas-consuming reactions is the influence of transport phenomena. The reaction partner hydrogen must be transported to the catalyst, and thereby it should penetrate the gas–liquid inter-

Fig. 10.3 Normal pressure hydrogenation device for the automatic registration of hydrogen consumption under isobaric conditions.

face at a distinctly higher rate than it is consumed by the hydrogenation. Only if such a regime holds it can be guaranteed that the detected effect can be interpreted as being exclusively kinetic.

Blackmond et al. investigated the influence of gas-liquid mass transfer on the selectivity of various hydrogenations [39]. It could be shown – somewhat impressively – that even the pressure-dependence of enantioselectivity of the asymmetric hydrogenation of α-dehydroamino acid derivatives with Rh-catalysts (as described elsewhere [21b]) can be simulated under conditions of varying influence of diffusion! These results demonstrate the importance of knowing the role of transport phenomena while monitoring hydrogenations.

Several possibilities exist to determine the influence of transport phenomena. The measurement of gas consumption in dependence on the interfacial area, the physical absorption coefficient, the rate of a chemical reaction following the absorption, and the concentration gradient (as the driving force of the absorption) allows decisions to be made on which regime is, in fact, in existence [40].

For the rate of physical absorption of a gas into a liquid without subsequent chemical reaction, Eq. (10) is valid.

$$\frac{d[C]}{dt} = k_L \cdot a \cdot ([C^*] - [C]) \quad \text{or} \quad [C] = [C^*] \cdot (1 - e^{-k_L \cdot a \cdot t}) \tag{10}$$

where k_L = physical mass-transfer coefficient (liquid side), a = interfacial area, $[C^*]$ = gas concentration in solution at time $t\infty$ (gas solubility), and $[C]$ = gas concentration in solution at time t.

The analysis of gas absorption proceeding exponentially under experimental conditions provides the gas solubility $[C^*]$ and the value of $k_L \cdot a$. As a rule of thumb, this value should be approximately ten-fold larger than the rate of a subsequent chemical reaction in order to eliminate diffusion influences on the latter reaction [41].

The often-applied method of determining the dependence of initial rate on stirring speed must be treated with caution, for two reasons. On the one hand, the initial rate can be lower than at higher conversions due to induction periods [42], and on the other hand an increase in stirring speed does not enforce a proportionally higher interfacial area.

The following procedure has been approved as being straightforward (also see [43]). A zero-order dependence is achieved by monitoring a reaction in the range of diffusion control. The rate is determined only by the constant concentration gradient in the interfacial area. The systematic investigation of whether diffusion influences hydrogenations is appropriate only if they also follow zero order, but in the range of kinetic control. An example of this is the catalytic hydrogenation of dienes as COD (cycloocta-1,5-diene) or NBD (norborna-2,5-diene) with cationic rhodium(I) chelates. Up to high conversions this reaction proceeds in the saturation range of Michaelis-Menten kinetics, and hence as a zero-order reaction. The pseudo-rate constant $k_{obs} = k_2' \cdot [H_2] \cdot [E]_0$ is a linear function of the initial catalyst concentration. A continuous increase of the employed catalyst concentration ($[E]_0$) under given experimental conditions (reactor geometry, stirring speed, stirrer size) leads to a straight line, and the hydrogen consumption is independent of the predominating regime (kinetics versus diffusion). Plotting the slopes of the straight lines as a function of the catalyst concentration provides information about the limitations of the regime, which is exclusively controlled by kinetics. Figure 10.4 illustrates the hydrogenation curves of the catalytic hydrogenation of NBD with $[Rh(Ph\text{-}\beta\text{-glup-OH})NBD]BF_4$ (Ph-β-glup-OH = phenyl 2,3-bis(*O*-diphenylphosphino)-β-D-glyco-pyranoside).

The plot of measured rates as a function of the initial catalyst concentration is shown in Figure 10.5. For the range from 0 to ca. 12 mL min^{-1} the straight line passing through the origin proves the direct proportionality between rate and catalyst concentration. In other words, the hydrogen concentration in solution (gas solubility) for the mentioned range of rates is constant, and it is measured in the kinetically controlled range. As the figure indicates, rates of hydrogen consumption of 30 mL min^{-1} are indeed nonproblematic with regard to the registration. However, for rates greater than 12 mL min^{-1}, gas consumption under the given experimental conditions is increasingly determined by transport phenomena. Because of the rising influence of diffusion, the bulk concentration of hydrogen in solution continuously decreases below the value of the hydrogen solubility. The hydrogenations are slower than would be expected for the kinetically controlled range.

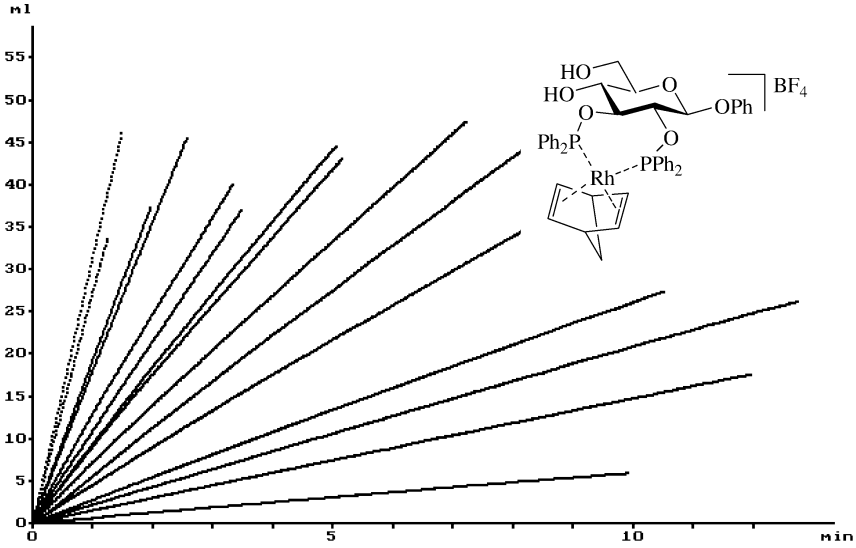

Fig. 10.4 Hydrogenation curves of catalytic NBD hydrogenations (each at least 2.0 mmol) with [Rh(Ph-β-glup-OH)NBD]BF_4 at varying catalyst concentrations (0.0025, 0.005, 0.0075, 0.01, 0.015, 0.02, 0.025, 0.03, 0.035, 0.04, 0.05, 0.08, 0.1, 0.15, and 0.2 mmol) each in 15.0 mL MeOH at 25.0 °C and 1.013 bar total pressure.

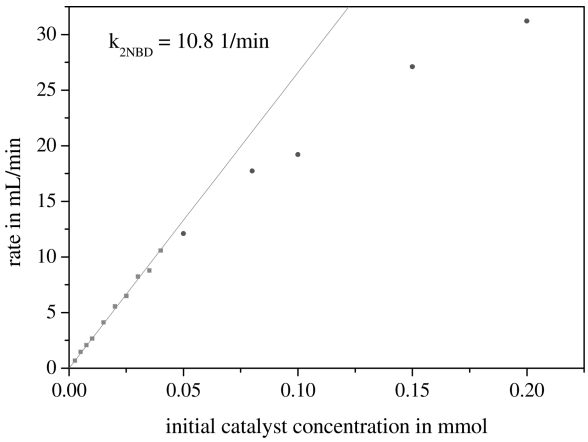

Fig. 10.5 Rate of gas consumption from Figure 10.4 as a function of initial catalyst concentration $[E]_0$.

One further source of error is that of vapor pressure of the solvent. Whilst this plays only a minor role at higher hydrogen pressures, its neglect for hydrogenations under normal pressure is a problem that is often underestimated. Figure 10.6 illustrates the vapor pressure of various solvents often used in hydrogenations as a function of temperature [44].

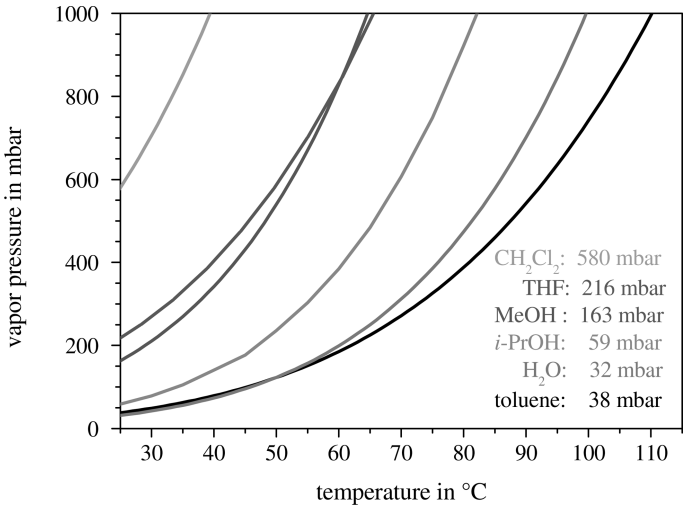

Fig. 10.6 Vapor pressure of CH_2Cl_2, THF, MeOH, *i*-PrOH, H_2O and toluene as a function of temperature. The concrete values refer to 25.0 °C.

Although in the case of methylene chloride under normal pressure more than one-half of the gas phase consists of solvent vapor (57%), in the case of toluene and water this share amounts to only ca. 3–4% of the total pressure. In order to compare activities in various solvents at the same hydrogen pressure above the reaction solution, besides a different gas solubility for the solvents (i.e., the hydrogen concentration in solution), a different partial pressure of hydrogen must be taken into account.

Another problem results from high vapor pressures of relatively low-boiling solvents. With regard to the dependence on reactor geometry, it can take some time for the vapor pressure of the solvent to become established in the gas phase of the closed system. As this equilibration of vapor pressure provides a positive volume contribution (the pressure above the reaction solution increases in a closed system), measured gas consumptions can be considerably falsified not only as a function of time but also in respect of the overall balance! One way to avoid this problem is to separate the gas phase above the reaction solution from the gas in the measuring burette by using a tempered bubble counter (cf. Fig. 10.3).

A further problem is constituted by the different solubilities of hydrogen in the conventional solvents used for hydrogenations. In Table 10.1 (column 2), data are listed of gas solubility (expressed as mole fraction) $[x_{H_2} = n_{H_2}/(n_{solvent} + n_{H_2})]$ of various solvents at 25.0 °C and 1.013 bar H_2 partial pressure [45].

Because very small mole fraction solubilities correspond in practice to the molar ratio [45a], the values can (considering the molar volume and density of the solvent) be easily transformed into hydrogen concentrations (see Table 10.1,

Table 10.1 Hydrogen solubilities in various solvents at 25.0 °C [46].

Solvent	H_2-solubility [mole fraction x at 1.013 bar]	Mol H_2 in 1 L solvent [1.013 bar H_2]	Mol H_2 "effective" in 1 L solvent [1.013 bar total pressure]
THF	0.000270	3.3291×10^{-3}	2.62×10^{-3}
MeOH	0.000161	3.9752×10^{-3}	3.33×10^{-3}
i-PrOH	0.000266	3.4742×10^{-3}	3.27×10^{-3}
H_2O	0.0000141	7.80576×10^{-4}	7.56×10^{-4}
Toluene	0.000317	2.9576×10^{-3}	2.85×10^{-3}

column 3). In hydrogenations under normal pressure, however, the different vapor pressure of the solvent, by which the relevant hydrogen partial pressure is reduced, must be taken into account (Fig. 10.6). Consideration of the vapor pressure of the solvent at a total pressure of 1.013 bar above the reaction solution leads to an "effective" gas solubility – that is the actually interesting hydrogen concentration in solution (see Table 10.1, column 4). The results show that under equal conditions (25.0 °C and 1.013 bar total pressure above the reaction solution), the hydrogen concentration in solution differs markedly for different solvents. The solvents THF and *i*-PrOH indeed show a similar hydrogen solubility (Table 10.1, column 2), despite differing in the "effective" hydrogen concentration (Table 10.1, column 4) by ca. 20%. In contrast, the solvents H_2O and toluene exhibit approximately the same vapor pressure above the reaction solution (Fig. 10.6), yet the "effective" hydrogen concentration in solution differs by a factor of 3.7. In the first case, variation in vapor pressure is the cause for such behavior, but in the second case it is the variation in gas solubility.

For meaningful comparisons of the activity of catalysts in various solvents under seemingly equal conditions these factors must, of course, be considered.

In order to determine the reaction order in hydrogen of a homogeneously catalyzed hydrogenation under isobaric conditions, the variation of partial pressure is an essential precondition. Commonly, hydrogen/inert gas mixtures are used, yet the change in composition of the gas mixture (the share of H_2 is reduced due to consumption in the hydrogenation) is generally neglected. However, this may lead to a dependence on the volume of the gas phase and, potentially, to a major systematic error. By contrast, the method described in the following section permits the use of isobaric conditions by varying the partial pressure.

While the gas phase above the reaction solution contains the reactive gas at a chosen concentration (obtained by dissolution with an inert gas such as argon; H_2/Ar gas mixtures are available commercially), pure hydrogen is arranged in the gas burette. Mixing of the gas phases, each of which has a different hydrogen concentration, is prevented by a bubble counter. After beginning the hydrogenation, hydrogen is delivered exclusively from the gas burette in order to obtain pressure equalization. The main problem with this type of measurement is that a concentration gradient (caused by the higher concentration of gas streaming into the

Fig. 10.7 An apparatus used to monitor hydrogenations at different hydrogen partial pressures.

gas space above the reaction solution) must be avoided. In addition to thorough mixing of the gas phase above the reaction solution, this problem could be solved by including an arrangement whereby the bubble counter between the gas volume above the reaction solution and the gas burette is located directly above the reaction solution in the gas phase of the hydrogenation vessel (cf. Fig. 10.7).

The result of the described methodical solution to monitor gas-consuming reactions at reduced partial pressure under isobaric conditions is shown in Figure 10.8 for the catalytic hydrogenation of COD with a cationic Rh-complex. The slope of the measured straight lines corresponds to the maximally obtainable rate ($V_{sat} = k_2 \cdot [E]_0 = k_2' \cdot [H_2] \cdot [E]_0$) [42b], which is directly proportional to the hydrogen concentration in solution and at validity of Henry's law to the hydrogen partial pressure above the reaction solution. The experiments prove that the "dilution factor" of the gas phase can adequately be found in the rate constant. (Further examples can be found in [47].)

Besides the above-mentioned errors, further difficulties may arise in the *in-situ* monitoring of hydrogenations. For example, in order to start a hydrogenation it is necessary to exchange inert gas and hydrogen by evacuation. In fact, this procedure leads to a cooling of the solution caused by the evaporation enthalpy of the solvent. The time taken to reach the equilibrium value of the vapor pressure of the solvent above the reaction solution must also be taken into account. In order to avoid such problems, it has been proven of value to seal the catalyst (or the substrate) in a glass ampoule under argon (cf. Fig. 10.3), and to start the hydrogena-

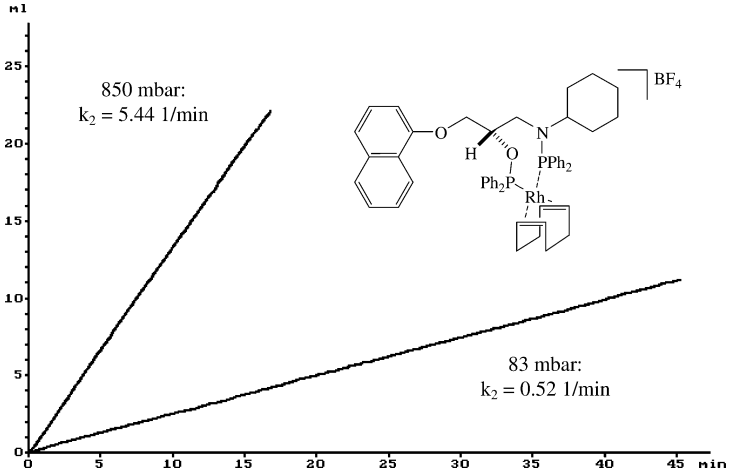

Fig. 10.8 Rate constant k_2 for the catalytic COD-hydrogenation with [Rh(cyclohexyl-PROPRAPHOS)COD]BF_4 as catalyst at various hydrogen partial pressures (normal pressure and commercial argon/hydrogen mixtures (AGA) which contain 9.71% H_2). Reaction mixture: 15.0 mL MeOH; 0.01 mmol catalyst; 1.0 mmol COD.

tion by destroying the ampoule only when the thermal equilibria have been established. It must be borne in mind, however, that it is extremely difficult to exclude all error sources, and at best a minimization of the problem is possible for a concrete case. However, it is important to assess – and at least report – the expected relative importance of those errors that have been neglected.

10.3.1.2 **Monitoring of Hydrogenations by NMR and UV/Visible Spectroscopy**

The details of a series of *in-situ* methods and appropriate investigations have been described concerning NMR spectroscopic monitoring of catalytic reactions with gases in various pressure ranges [42e, 48]. However, disadvantages might include the reactive gas not being supplied, that isobaric conditions during the gas consumption are not possible, that thorough mixing of the reaction solution is insufficient (diffusion problems), or that special NMR probe heads are necessary. A very interesting solution has been described by Iggo et al. [48d], in which the NMR flow cell for the *in-situ* study of homogeneous catalysis allows measurements up to 190 bar (!), but requires the use of a standard wide-bore NMR probe. Details of state-of-the-art methods for the *in-situ* monitoring of reactions using NMR spectroscopy can be found in [49].

An improvement of the possibility for experiments under normal pressure (as described in [42e]) is shown in Figure 10.9 [50]. During registration of the spectrum, the reactive gas is continuously bubbled into the reaction solution below the NMR-active sample volume; thus, diffusion problems can be excluded for mod-

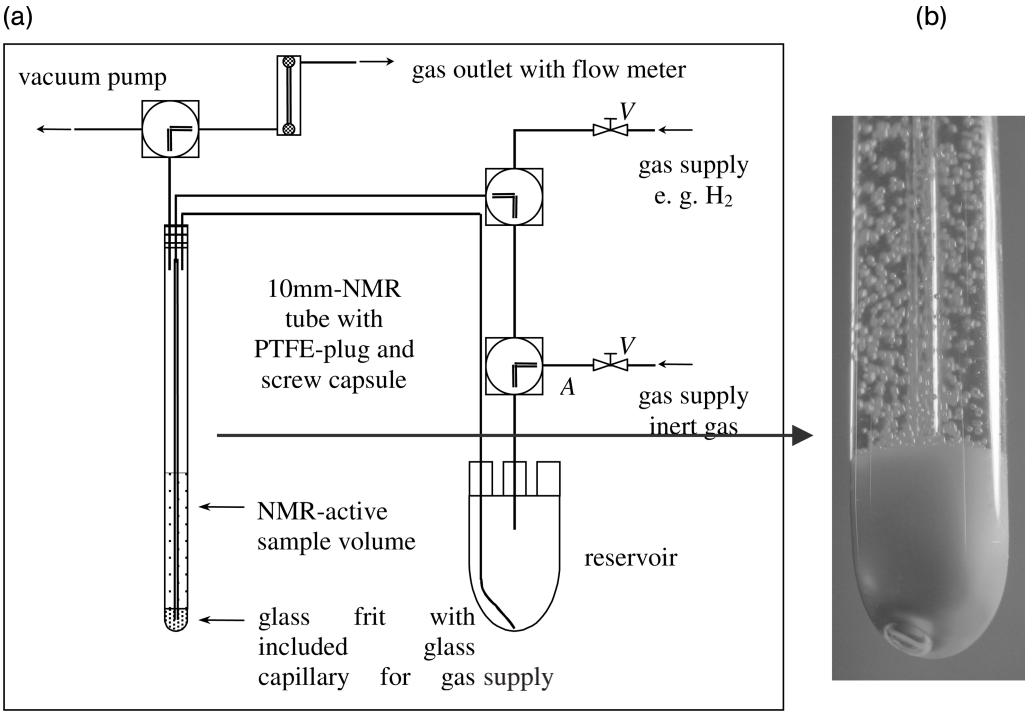

Fig. 10.9 (a) Schematic arrangement for the NMR-spectroscopic monitoring of gas-consuming reactions under catalytic conditions according to [50]. (b) Gas flow during the measurement (a – argon, b – hydrogen).

erately fast reactions. In spite of the introduction of gas during the measurement (cf. Fig. 10.9 b) and hence a deterioration in the homogeneity of the magnetic field, sufficiently good spectra (^{1}H, ^{13}C, ^{31}P) can be obtained under *in-situ* catalytic conditions using the non-rotating NMR tube. One disadvantage of this arrangement is that the gas excess is withdrawn from the device and disappears. For this reason, it is not economical to employ expensive, isotopically labeled gaseous reaction partners such as $^{2}H_2$ and ^{13}CO. Moreover, because of the permanent loss of gas – especially in long-term measurements – the solvent is also discharged.

An application of the arrangement shown in Figure 10.9 is depicted in Figure 10.10. For the hydrogenation of (*Z*)-*N*-acetylamino methyl cinnamate (AMe) with [Rh(DIPAMP)(solvent)$_2$]anion (DIPAMP = 1,2-bis-(*o*-methoxy-phenyl-phenyl phosphino)ethane) in isopropyl alcohol at 25 °C and under normal pressure, the ^{31}P-NMR spectrum shown in Figure 10.10 b was measured during hydrogenation under steady-state conditions. The comparison with the spectrum taken under argon (Fig. 10.10 a) proves that the ratio major/minor catalyst–substrate complex is higher during the hydrogenation than under thermodynamic conditions (argon). The measurement of a similar spectrum after termination of hydrogen supply and in-

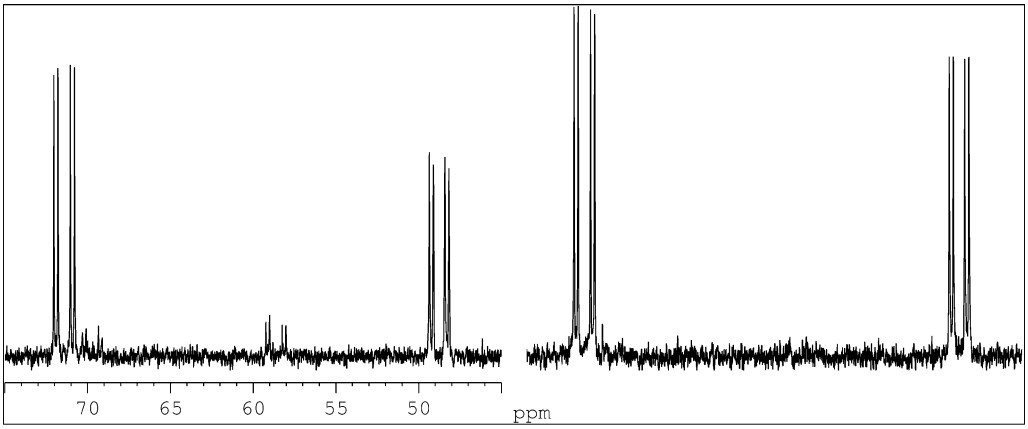

Fig. 10.10 ^{31}P-NMR spectra of $[Rh(DIPAMP)(MeOH)_2]^+$ and 1.0 mmol AMe in 5.0 mL iso-propyl alcohol-d_8 at 25 °C with the arrangement shown in Figure 10.9. Spectrum (a) is registered under argon; spectrum (b) is accumulated during a reaction time of 30 min (1200 pulses).

troduction of argon virtually congruently leads to the initial spectrum. Thus, it could clearly be proven that the change in the phosphorus spectra should be exclusively attributed to the reaction with hydrogen.

Recently, a new (and now commercially available) methodology was reported for measuring *in-situ* high pressure NMR spectra up to 50 bar under stationary conditions. The instrument uses a modified sapphire NMR tube, and gas saturation of the sample solution and exact pressure control is guaranteed throughout the overall measurement, even at variable temperatures. For this purpose, a special gas cycling system is positioned outside the magnet in the routine NMR laboratory [51].

Today, stirring inside UV/visible cells, cell tempering, the use of flow-through cells, and the detection of smallest amounts of samples in microcells are all possible, without problems. However, a complete gas exchange (e.g., argon for hydrogen) is still difficult. Moreover, because of the disadvantageous geometry of a cell in terms of the ratio of surface to volume, it is generally only possible to trace relatively slow reactions with gases in the kinetically controlled regime. After all, the realization of isobaric conditions for the gaseous reaction partner in case of a cell represents high requirements to the pressure adjustment since the gas consumptions are relatively small. For such problems, the application of immersion probes (known also as "fiber-optical probes") represents a good alternative. Due to the arbitrary dimensioning of the reaction vessel and the immersion probe (an example for analyses under normal pressure is shown in Fig. 10.11), hydrogenations can be monitored *in situ* over a variety of pressure and temperature ranges, and in an elegant manner.

The "external" measurement of UV/visible spectra principally allows the tracing of other quantities at the same time, such as conductivity, pH, and gas con-

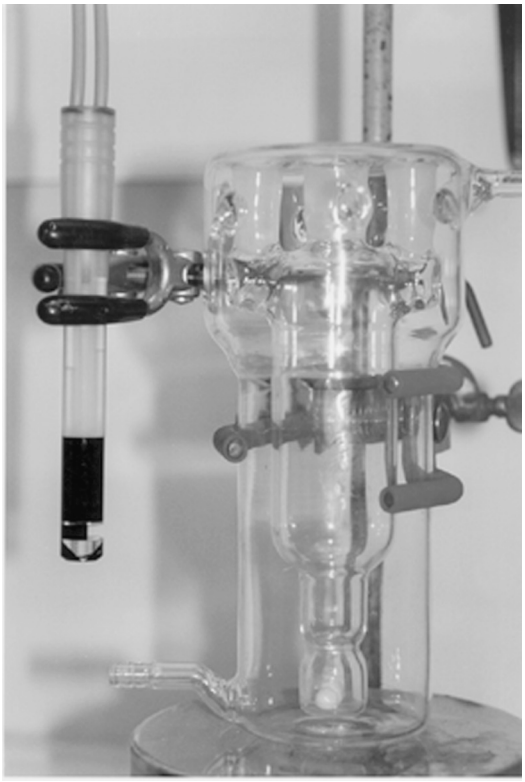

Fig. 10.11 Immersion probe with standard ground joint and reaction vessel for UV/visible spectroscopic analyses under normal pressure.

sumption under catalytic conditions. Monitoring of the time-dependent change of extinction at the maximum (441 nm) of [Rh(DIOP)(COD)]BF_4 (DIOP = 4,5-bis(diphenyl-phosphino-methyl)-2,2-dimethyl-1,3-dioxolane)] for the catalytic hydrogenation of COD and the simultaneous registration of hydrogen consumption is shown graphically in Figure 10.12.

The rate constant can be obtained directly from the slope of the graph [42f]. Furthermore, it can clearly be seen that the concentration of [Rh(DIOP)(COD)]BF_4, both under argon and during the hydrogenation, is the same until depletion of the substrate COD. This confirms that hydrogenation proceeds in the range of saturation kinetics of the underlying Michaelis-Menten kinetics. Thus, the experimental procedure provides information regarding the catalyst via UV/visible spectroscopy; subsequently, the rate of product formation can be quantified from the hydrogen consumption of the very same reaction solution [52].

In addition to the above-mentioned possibilities for the *in-situ* monitoring of hydrogenations, there are, of course, also techniques involving calorimetry and IR spectroscopy [34, 35c, 39, 41, 53, 54].

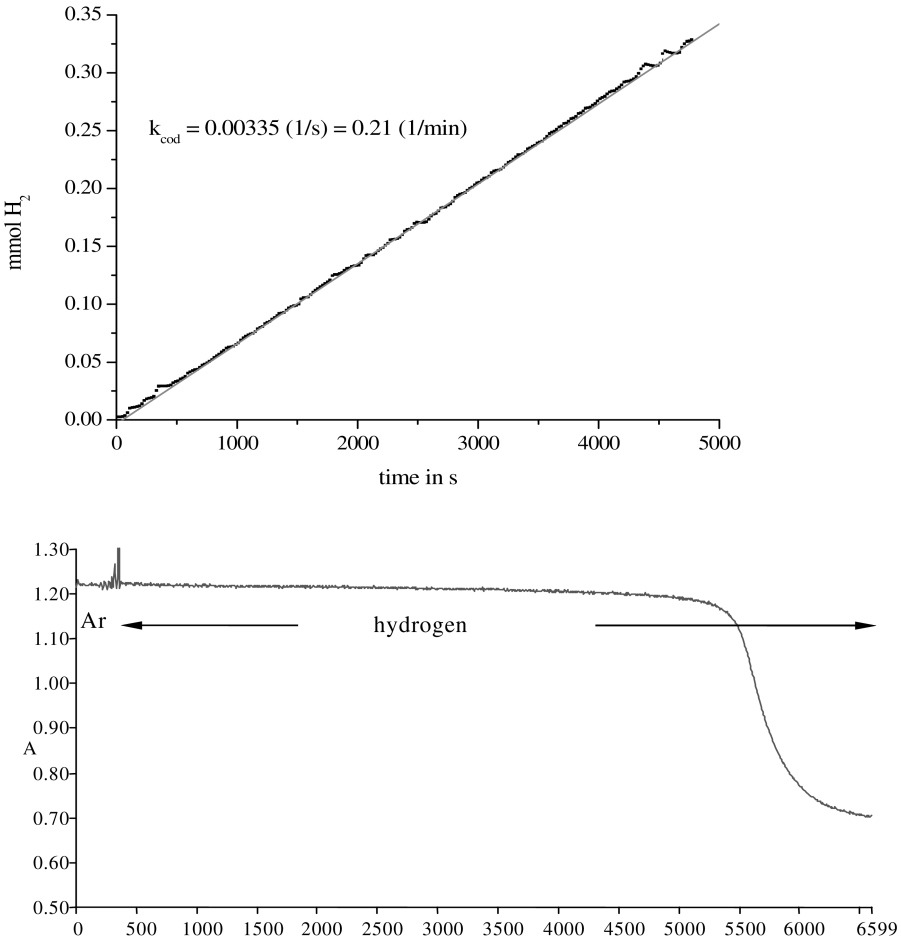

Fig. 10.12 Simultaneous monitoring of the time-dependent UV/visible spectrum at 441 nm (maximum of the catalyst extinction) and hydrogen consumption for the hydrogenation of COD with [Rh(DIOP)COD]BF_4. Conditions: 0.02 mmol precatalyst; 0.33 mmol COD; 20.0 mL methanol; 25.0 °C; 1.013 bar total pressure.

10.3.2 Gross-Kinetic Measurements

10.3.2.1 Derivation of Michaelis-Menten Kinetics with Various Catalyst-Substrate Complexes

The catalytic asymmetric hydrogenation with cationic Rh(I)-complexes is one of the best-understood selection processes, the reaction sequence having been elucidated by Halpern, Landis and colleagues [21a, b], as well as by Brown et al. [55]. Diastereomeric substrate complexes are formed in pre-equilibria from the solvent complex, as the active species, and the prochiral olefin. They react in a series of elementary steps – oxidative addition of hydrogen, insertion, and reductive elimination – to yield the enantiomeric products (cf. Scheme 10.2) [56].

The rate law for two diastereomeric catalyst–substrate complexes (C_2-symmetric ligands) resulting from Michaelis-Menten kinetics (Eq. (11)) has already been utilized by Halpern et al. for the kinetic analysis of hydrogenations according to Scheme 10.2, and corresponds to Eq. (3) of this study.

$$\frac{d[H_2]}{dt} = \frac{d[R]}{dt} + \frac{d[S]}{dt} = \frac{\left(\frac{(k_{2min} \cdot K_{ESmin}) + (k_{2maj} \cdot K_{ESmaj})}{K_{ESmin} + K_{ESmaj}}\right) \cdot [Rh]_0 \cdot [olefine]}{\left(\frac{1}{K_{ESmin} + K_{ESmaj}}\right) + [olefine]}$$

with

$$K_{ESmin} = \frac{k_{1min}}{k_{-1min} + (k_{2min} \cdot [H_2])} \quad K_{ESmaj} = \frac{k_{1maj}}{k_{-1maj} + (k_{2maj} \cdot [H_2])} \tag{11}$$

In answer to the question, "why are there not much more kinetic analyses of selection processes in analogy to these classic works?", it should be realized that particular prerequisites are necessary. In the concrete case, such prerequisites included a major stability of the substrate complexes, a convenient ratio of the diastereomeric substrate complexes, and a pressure-dependence of the enantioselectivities.

The following section deals with kinetic equations for the simple Michaelis-Menten kinetics with more than two intermediates; subsequently, their application for the interpretation of hydrogenations in practical examples is discussed.

If C_1-symmetric ligands are employed in asymmetric hydrogenation instead of the corresponding C_2-symmetric ligands, there coexist principally four stereoisomeric substrate complexes, namely two pairs of each diastereomeric substrate complex. Furthermore, it has been shown that, for particular catalytic systems, intramolecular exchange processes between the diastereomeric substrate complexes should in principle be taken into account [57]. Finally, the possibility of non-established pre-equilibria must be considered [58]. The consideration of four intermediates, with possible intramolecular equilibria and disturbed pre-equilibria, results in the reaction sequence shown in Scheme 10.3. This is an example of the asymmetric hydrogenation of dimethyl itaconate with a Rh-complex, which contains a C_1-symmetrical aminophosphine phosphinite as the chiral ligand.

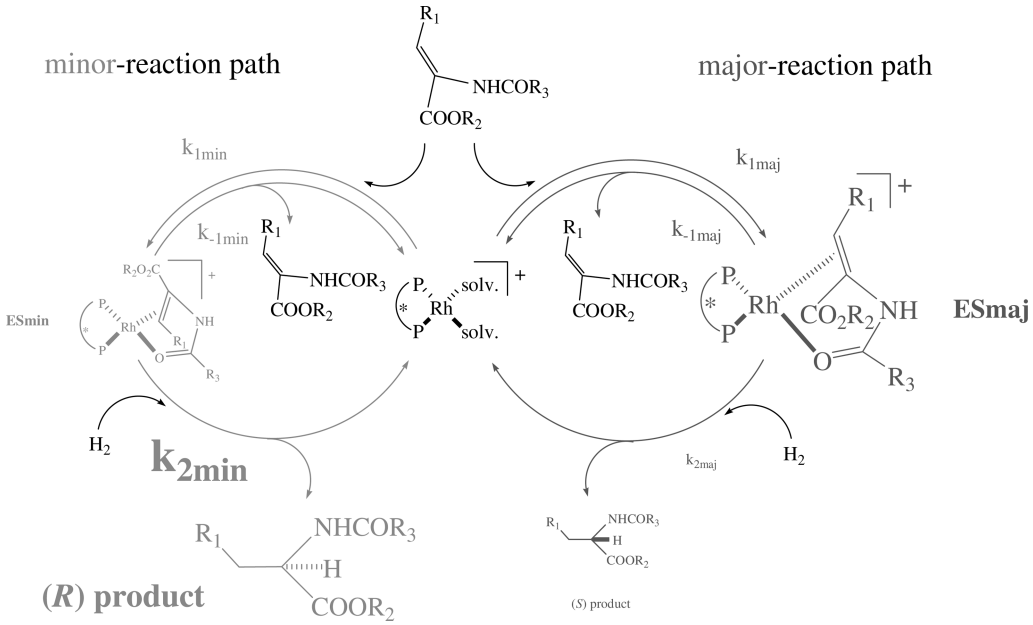

Scheme 10.2 Selection model of the Rh(I)-complex-catalyzed asymmetric hydrogenation to the (*R*)-amino acid derivative (according to [21a, b, 55]). ES_{maj} and ES_{min} correspond to the diastereomeric catalyst–substrate complexes.

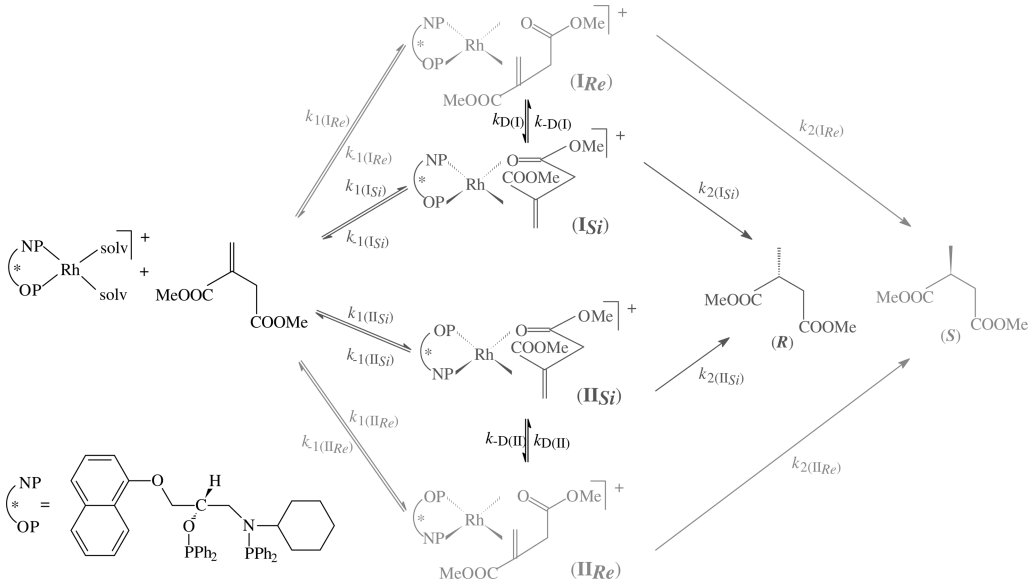

Scheme 10.3 Reaction sequence for the asymmetric hydrogenation of dimethyl itaconate with a C_1-symmetric ligand under consideration of intramolecular exchange processes between the intermediates and of disturbed pre-equilibria.

For the time-dependent change of the particular concentrations, Eqs. (12a) and (12b) result.

$$\text{(a)}\ \frac{d[S]}{dt} = k_{2(I_{Re})} \cdot [I_{Re}] + k_{2(II_{Re})} \cdot [II_{Re}] \quad \text{(b)}\ \frac{d[R]}{dt} = k_{2(I_{Si})} \cdot [I_{Si}] + k_{2(II_{Si})} \cdot [II_{Si}] \tag{12}$$

The common further treatment of the approach – assumption of steady-state conditions for the intermediate substrate complexes, consideration of the catalyst balance ([catalyst]$_0$ = [solvent complex] + [I_{Re}] + [I_{Si}] + [II_{Re}] + [II_{Si}]) and of the stoichiometry of the hydrogenation – provides the rate of hydrogen consumption under isobaric conditions (Eq. (13)) [57f]. A more general derivation can be found in [59].

$$\begin{aligned} -\frac{d[H_2]}{dt} &= \frac{d[S]}{dt} + \frac{d[R]}{dt} \\ &= \frac{\dfrac{(k_{2(I_{Re})} \cdot K_{I_{Re}} + k_{2(II_{Re})} \cdot K_{II_{Re}} + k_{2(I_{Si})} \cdot K_{I_{Si}} + k_{2(II_{Si})} \cdot K_{II_{Si}})}{(K_{I_{Re}} + K_{I_{Si}} + K_{II_{Re}} + K_{II_{Si}})} \cdot [cat]_0 \cdot [S]}{\dfrac{1}{(K_{I_{Re}} + K_{I_{Si}} + K_{II_{Re}} + K_{II_{Si}})} + [S]} \\ &= \frac{k_{obs} \cdot [cat]_0 \cdot ([S]_0 - n_{H_2})}{K_M + ([S]_0 - n_{H_2})} \end{aligned} \tag{13}$$

This relationship corresponds to the simplest Michaelis-Menten kinetics (Eq. (3)). In addition to the equation derived earlier by Halpern et al. for the simplest model case of a C_2-symmetric ligand without intramolecular exchange [21b], every other possibility of reaction sequence corresponding to Scheme 10.3 can be reduced to Eq. (13). Only the physical content of the values of k_{obs} and K_M, which must be determined macroscopically, differs depending upon the approach (see [59] for details). Nonetheless, the constants k_{obs} and K_M allow conclusions to be made about the catalyses:

- The value $1/K_M$ corresponds to the ratio of concentrations of the sum of all catalyst–substrate complexes to the product {[solvent complex]·[substrate]}, and thus is a measure of how much catalyst–substrate complex is present [60].
- The k_{obs}-values are all to be interpreted as the sum of all rate constants for the oxidative addition of hydrogen, each multiplied by the mole fraction of the corresponding catalyst–substrate complex. Hence this "gross-rate constant" is dependent only on the ratio of intermediates, and not on their absolute concentrations.

Clearly, a comprehensive description of catalytic systems is not possible from the hydrogen consumption alone. The reaction sequence represented in Scheme 10.3 already contains 16 rate constants. However, valuable data regarding the catalysis can be obtained from an analysis of the gross hydrogen consumption on the basis of Eq. (13), for various catalytic systems. Some practical examples of this are described in the following section.

10.3.2.2 Data from Gross Kinetic Measurements

The hydrogen consumption and enantioselectivities for the asymmetric hydrogenation of dimethyl itaconate with various substituted catalysts of the basic type [Rh(PROPRAPHOS)COD]BF_4 are illustrated in Figure 10.13 [61]. The systems are especially suitable for kinetic measurements because of the rapid hydrogenation of COD in the precatalyst. There are, in practice, no disturbances due to the occurrence of induction periods.

NMR-analyses suggest that the hydrogenation runs corresponding to Scheme 10.3. Three of the four possible catalyst–substrate complexes are detectable in the ^{31}P-NMR-spectrum [57f].

A comparison of the activities for various catalyst derivatives shown in Figure 10.13 seems to prove that the ligand with the cyclohexyl residue leads to the most active catalyst for the hydrogenation of dimethyl itaconate. The catalyst containing the methyl derivative apparently exhibits the lowest activity.

A more detailed analysis, however, shows that such comparisons of activity can be completely misleading, because Michaelis-Menten kinetics are principally described by two constants. The Michaelis constant contains information regarding the pre-equilibria, the rate constants quantify the product formation from the intermediates.

An analysis of the hydrogenation curves shown in Figure 10.13 indicates, for those precatalysts with R=2-propyl, 3-pentyl and cyclopentyl, that they can be described quantitatively as first-order reactions. The comparison between experimental and calculated data (the latter being determined by least-squares regres-

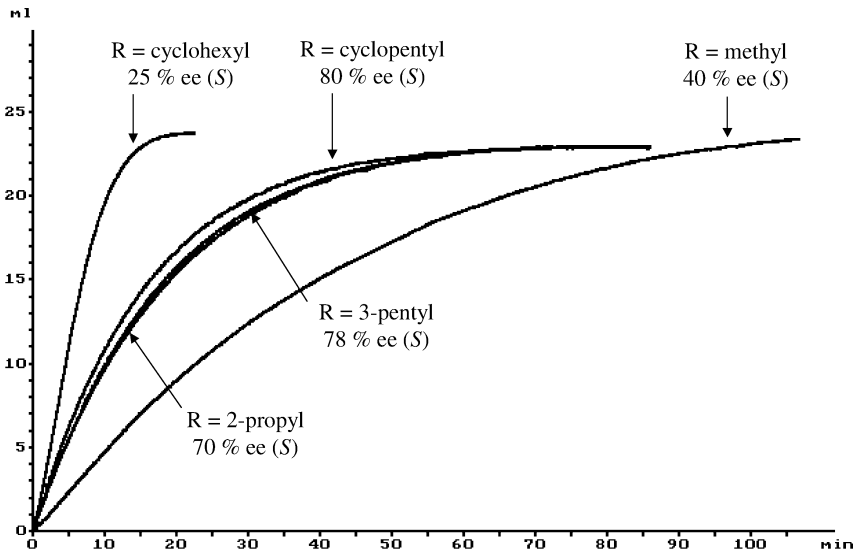

Fig. 10.13 Catalytic asymmetric hydrogenation of 1.0 mmol dimethyl itaconate with 0.01 mmol [Rh(PROPRAPHOS)COD]BF_4-precatalysts ((*S*)-PROPRAPHOS: R=2-propyl) in 15.0 mL MeOH at 1.013 bar total pressure and 25 °C.

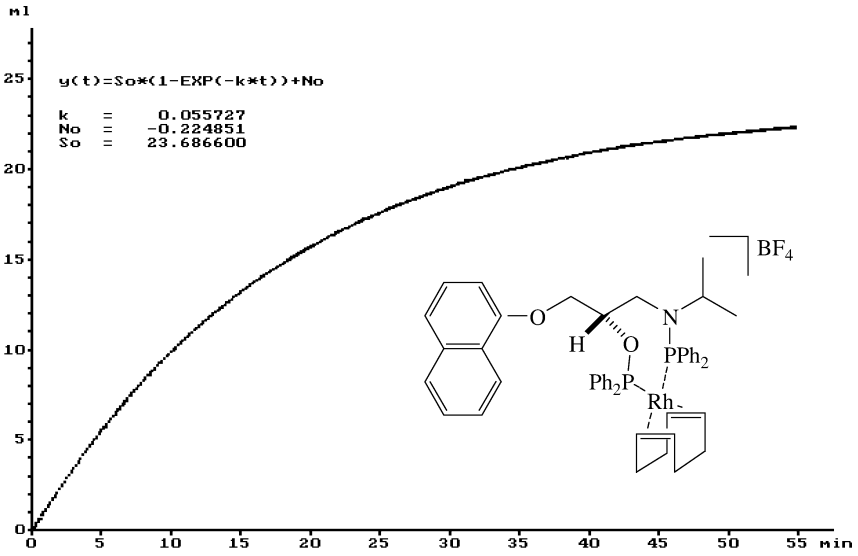

Fig. 10.14 Comparison of the experimental hydrogenation curve and first-order calculated values for the asymmetric hydrogenation of the PROPRAPHOS-precatalyst with dimethyl itaconate.

sion analysis) is shown in Figure 10.14. Due to the excellent conformity, these curves lie on top of each other.

If the ligands containing R = methyl and R = cyclohexyl are employed, the hydrogenations describe not only the initial range of the Michaelis-Menten equation, but also a range which cannot be assigned to the limiting case of the first-order reaction (cf. Figs. 10.1 and 10.2). Determination of the sought constants is carried out using nonlinear regression, with the initial values determined by linearization of Eq. (7). The comparison between experimental and calculated values corresponding to Eq. (13) for the ligand containing the methyl residue is shown in Figure 10.15. The results prove a good correspondence between the experiment and the model. For the initial quantity of substrate (1.0 mmol), the range of half-saturation concentration is reached almost at the start of the hydrogenation (Fig. 10.15).

The results of the kinetic analysis for the investigated systems are summarized in Table 10.2, the substrate concentration used being the same for all trials. In the case of methyl- and cyclohexyl-substituted ligands the Michaelis constant is smaller than the initial substrate concentration of $[S]_0 = 0.06666$ mol L^{-1} (Table 10.2). However, a description of the hydrogenations with other catalyst ligands as first-order reactions shows that in each of these cases the Michaelis constant must be much greater than the experimentally chosen substrate concentration.

Even at a rather higher substrate concentration, the limiting value of a concentration-independent rate is not reached in these cases. This is illustrated for the example of the PROPRAPHOS-type catalyst in Figure 10.16. It is, further-

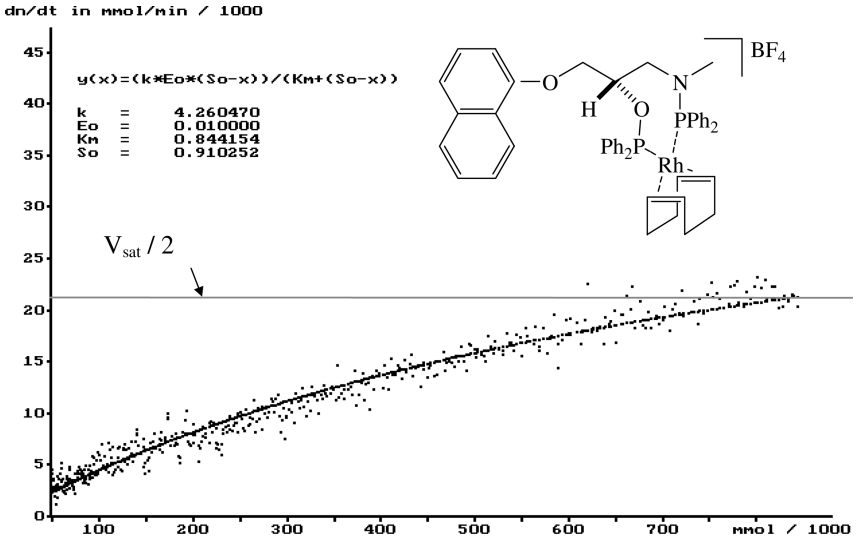

Fig. 10.15 Comparison of experimental and calculated values for the asymmetric hydrogenation of dimethyl itaconate with the methyl substituted ligand of the PROPRAPHOS precatalyst. Specifications of concentration refer to 15.0 mL of solvent.

Table 10.2 Kinetic analysis of the asymmetric hydrogenation of dimethyl itaconate with derivatives of [Rh(PROPRAPHOS)-COD]BF_4 (see Fig. 10.13).

Ligand	% ee	k (1st order) [1 s^{-1}]	K_M [mol L^{-1}]	$1/K_M$ [L mol^{-1}]	k_{obs} (Eq. (13)) [1 s^{-1}]	V_{sat} [mol L^{-1} s]
R = cyclohexyl	25	7.27×10^{-3}	0.0286	35	3.12×10^{-1}	2.08×10^{-4}
R = methyl	40	8.42×10^{-4}	0.0562	18	7.10×10^{-2}	4.73×10^{-5}
R = 2-propyl	70	9.28×10^{-4}	–	–	–	–
R = 3-pentyl	78	8.50×10^{-4}	–	–	–	–
R = cyclopentyl	80	1.07×10^{-3}	–	–	–	–

more, remarkable that at an increase in the substrate/catalyst ratio from 100 (standard conditions) to 1000 the PROPRAPHOS catalyst already shows an initial rate which is more than twice the maximum reachable rate with the cyclohexyl derivative (4.2×10^{-4} mol L^{-1} s versus 2.1×10^{-4} mol L^{-1} s). Indeed, PROPRAPHOS is still not used optimally with regard to its activity (see Fig. 10.16).

Interpretation of the reciprocals of the Michaelis constants allows the following conclusions to be made regarding hydrogenations under specified experimental conditions. In the case of the methyl and cyclohexyl ligand, the prevailing form of the catalyst in solution is the catalyst–substrate complex. However, for the other examples of first-order reactions, large Michaelis constants (or very

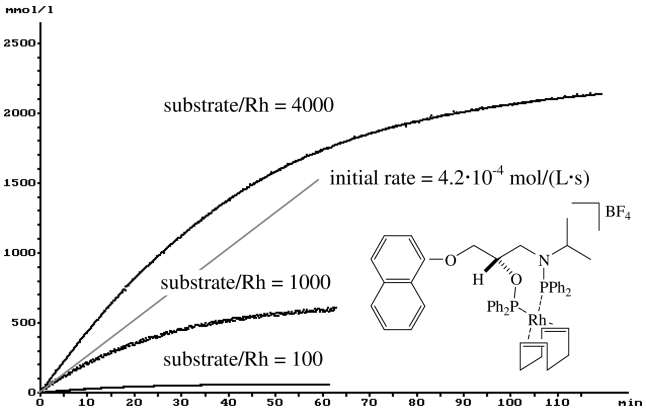

Fig. 10.16 Variation of the concentration of dimethyl itaconate for the hydrogenation with [Rh((*S*)-PROPRAPHOS)COD]BF_4.

small reciprocals of the same) prove that in these cases the equilibrium between solvent complex and the diastereomeric catalyst–substrate complexes is shifted to the side of the solvent complex.

These results, obtained from the gross-hydrogen consumption under normal conditions on the basis of the model developed above, make it clear that even catalysts of the same basic type can give rise to considerably different pre-equilibria. As a consequence, comparison of activities of various catalytic systems under "standard conditions" can provide the wrong picture. Hence, the cyclohexyl precatalyst with dimethyl itaconate seems to be the most active one (by reference to Fig. 10.13). Nonetheless, an increase in the initial substrate concentration by a factor of ten already leads to a different order in activity.

In addition to comparisons of activity of various catalysts, the choice of an appropriate solvent represents yet another problem in catalysis. The choice is usually made by direct comparison of the activity of a catalyst in various solvents. Nonetheless, analogous problems as mentioned above must be considered. Variable substrate concentrations can lead to seemingly different orders in the activity of solvents. The reason for this is based on the fact that macroscopic activity is caused by different amounts of catalyst–substrate complex.

These results underline the fact that "gross-activities" based on TOFs or half-lives only are not appropriate to compare catalytic systems that are characterized by pre-equilibria. Rather, only an analysis of gross-kinetics on the basis of suitable models can provide detailed information concerning the catalysis.

As explained earlier, the pre-equilibria are characterized by the limiting values of Michaelis-Menten kinetics. In the case of first-order reactions with respect to the substrate, we have: $K_M >> [S]_0$. Since the pre-equilibria are shifted to the side of educts during hydrogenation, only the solvent complex is detectable. In contrast, in the case of zero-order reactions only catalyst–substrate complexes are expected under stationary hydrogenation conditions in solution. These consequences resulting from Michaelis-Menten kinetics can easily be proven by var-

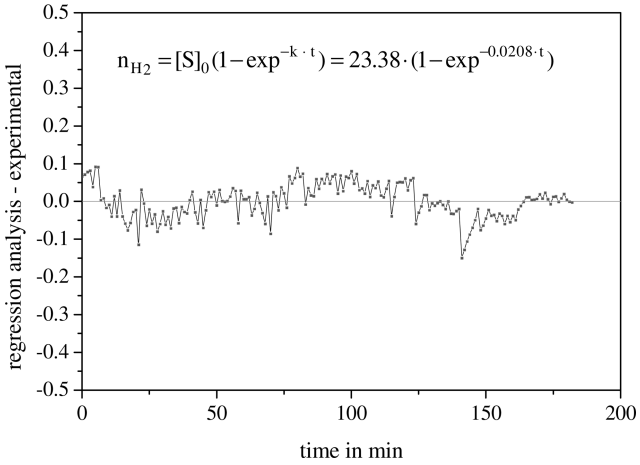

Fig. 10.17 Asymmetric hydrogenation of dimethyl itaconate with [Rh(Ph-*β*-glup-OH)(MeOH)$_2$]BF$_4$; comparison between first-order fit (x-axis) and experimental values. Conditions: 0.01 mmol catalyst; 1.0 mmol substrate; 15.0 mL MeOH; 1.013 bar total pressure.

ious methods such as NMR- and UV/visible spectroscopy, and this is demonstrated by some examples in the following section.

The asymmetric hydrogenation of dimethyl itaconate with [Rh(Ph-*β*-glup-OH-MeOH)$_2$]BF$_4$ runs as a first-order reaction. The deviation of experimental values from the hydrogen consumption calculated from parameters of nonlinear regression analysis (x-axis) is shown in Figure 10.17. In solution, only the solvent complex should be detectable during hydrogenation. In order to monitor hydrogenation via UV/visible spectroscopy, a 100-fold excess of the prochiral olefin is added to the solvent complex. The exchange of argon for hydrogen starts the hydrogenation, which is then monitored by cyclic measurement of the spectra (Fig. 10.18).

Although the substrate complexes absorb in the range of measurement (see Fig. 10.18, inset), the spectra observed during hydrogenation do not differ from the spectrum of the pure solvent complex. On completion of the reaction, gas chromatographic analysis proves that hydrogenation has occurred and that the usual values for conversion and selectivity have resulted. Thus, only solvent complex is present during the hydrogenation, and this corresponds to expectations from kinetic interpretations of the hydrogen consumption curve.

NMR spectroscopy provides analogue results. Inspection of hydrogen consumption curves following the hydrogenation of *Z*- or *E*-methyl 3-acetamidobutenoate with [Rh(Et-DuPHOS)(MeOH)$_2$]BF$_4$ (Et-DuPHOS = 1,2-bis(2,5-diethylphospholanyl)benzene)) showed the reaction to exhibit first-order kinetics (Fig. 10.19).

For both cases in these examples only the solvent complex is detectable, besides traces of non-hydrogenated COD-precatalyst (cf. Fig. 10.20).

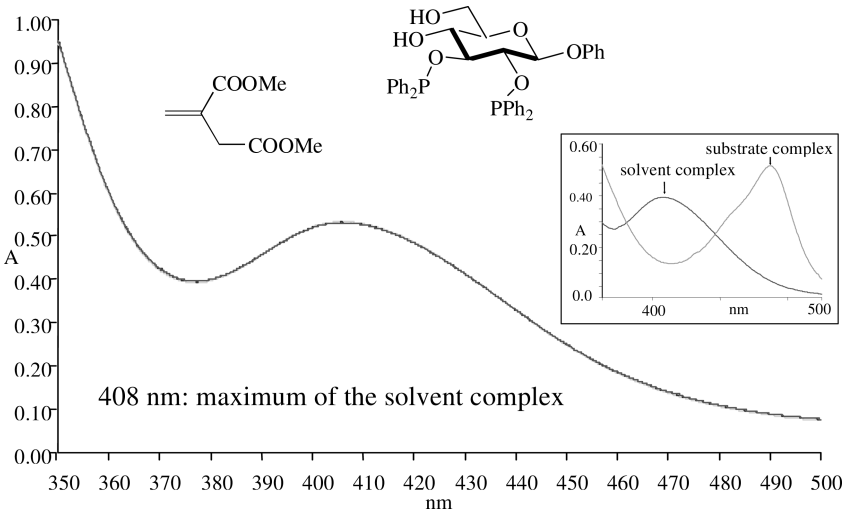

Fig. 10.18 UV/visible spectrum of 0.02 mmol [Rh(Ph-*β*-glup-OH)(MeOH)$_2$]BF$_4$ in 35.0 mL MeOH under Ar, and five spectra (cyclic, monitored at 6.0 min intervals) after addition of a 100-fold excess of dimethyl itaconate and exchange of Ar for H_2. Inset: the spectrum of the catalyst–substrate complex. GC analysis after 30 min hydrogenation: 45% conversion, 78% ee (*R*), which agrees well with corresponding hydrogenations.

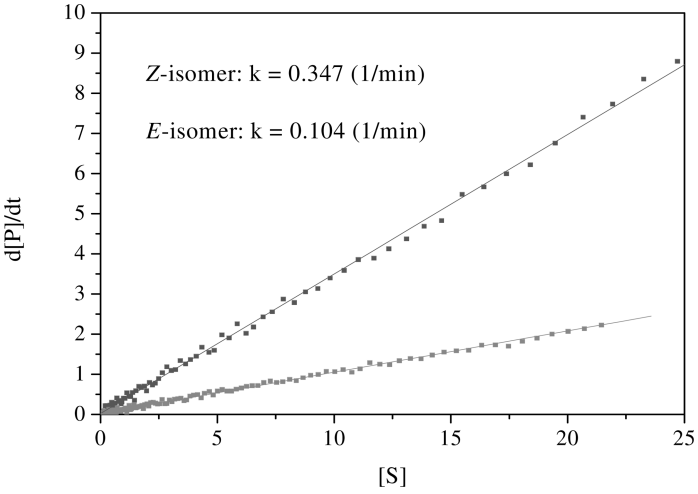

Fig. 10.19 Asymmetric hydrogenation of *E*- and *Z*-methyl 3-acetamidobutenoate with [Rh(Et-DuHOS)MeOH$_2$)]BF$_4$ as first-order reactions; d[P]/d*t* versus [S] (Eq. (4b)).

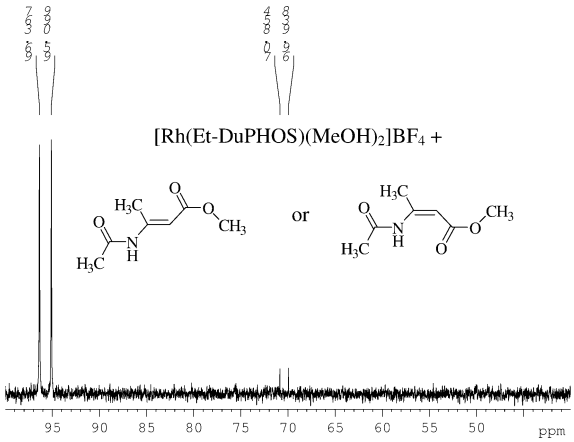

Fig. 10.20 ^{31}P-NMR spectrum of a solution of 0.01 mM [Rh(Et-DuPHOS)(MeOH)$_2$]BF$_4$ and 0.1 mM *E*- or *Z*-methyl 3-acetamidobutenoate.

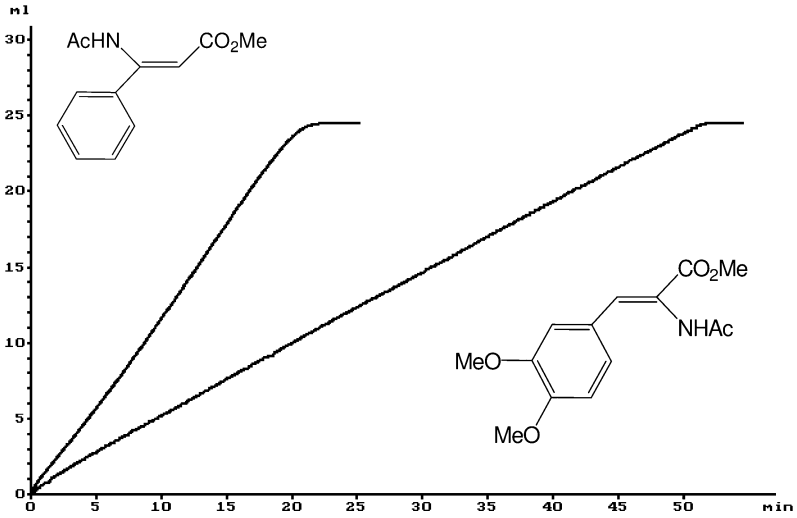

Fig. 10.21 Hydrogen consumption for the hydrogenation of (*Z*)-3-*N*-acetylamino-3-(phenyl)-methyl propenoate with [Rh((*R*,*R*)-Et-DuPHOS)(MeOH)$_2$]BF$_4$ in *i*-PrOH (59% ee) and (*Z*)-2-benzoylamino-3-(3,4-dimethoxy phenyl)-methyl acrylate with [Rh((*S*,*S*)-DIPAMP)(MeOH)$_2$]BF$_4$ in MeOH (98% ee). Conditions: 0.01 mmol catalyst; 1.0 mmol substrate; 15.0 mL solvent; 1.013 bar total pressure.

Nonetheless, if zero-order reactions are analyzed in terms of the validity of Michaelis-Menten kinetics, all of the catalyst is present in solution as catalyst–substrate complex up to high conversions. The hydrogenation rate is independent of the substrate concentration; two such examples are provided in Figure 10.21.

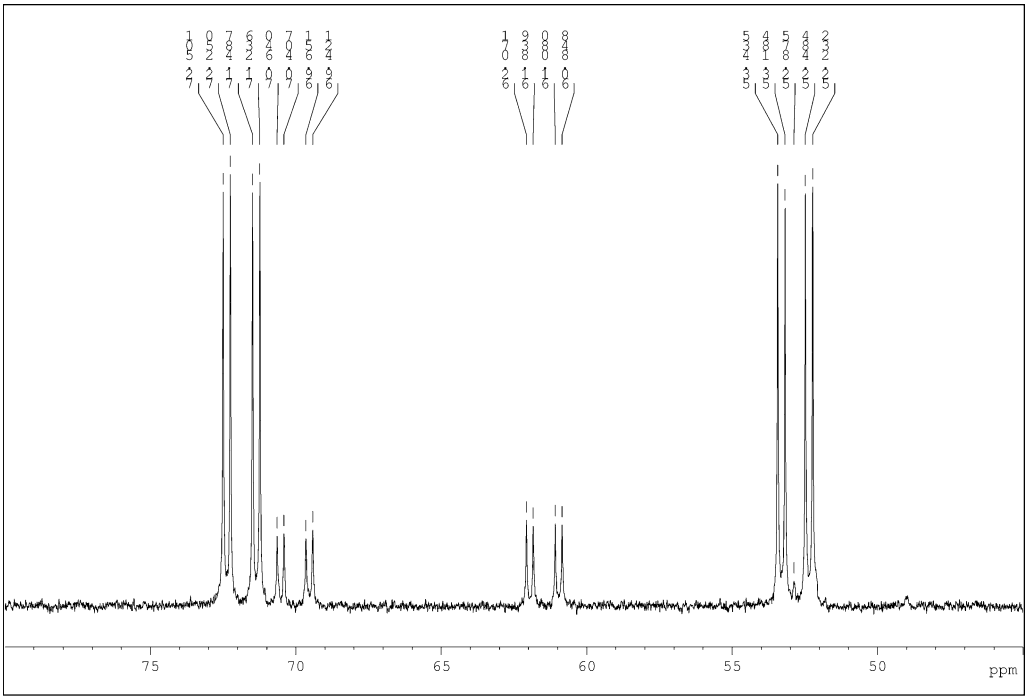

Fig. 10.22 ^{31}P-NMR spectrum of a solution of 0.02 mM [Rh((*S*,*S*)-DIPAMP)(MeOH)$_2$]BF_4 and 0.1 mM (*Z*)-2-benzoyl-amino-3-(3,4-dimethoxyphenyl)-methyl acrylate.

In these cases, the ^{31}P-NMR spectrum exhibits only signals of substrate complexes; there is almost no solvent complex visible. This is illustrated for (*Z*)-2-benzoylamino-3-(3,4-dimethoxyphenyl)-methyl acrylate with [Rh((*S*,*S*)-DIPAMP)(MeOH)$_2$]BF_4 in Figure 10.22.

Thus, if information is being sought about intermediates for this type of catalysis, it does not make sense to analyze systems that lead to first-order reactions! Rather, systems in which the hydrogenation rate is independent of the substrate concentration would be more appropriate. Indeed, for both catalytic systems shown in Figure 10.21, in each case one of the catalyst–substrate complexes could be isolated and characterized by crystal structure analysis (Fig. 10.23).

In the case of the α-dehydroamino acid (Fig. 10.23, right), it could be shown by using low-temperature NMR spectroscopy that the isolated crystals correspond to the major substrate complex in solution. However, according to the major–minor concept (see Scheme 10.2), it does not lead to the main enantiomer [63]. On the contrary, it could be proven unequivocally for various substrate complexes with β-dehydroamino acids that the isolated substrate complexes are major-substrate complexes. Surprisingly, they also gave the main enantiomer of the asymmetric hydrogenation, which would not be expected on the basis of

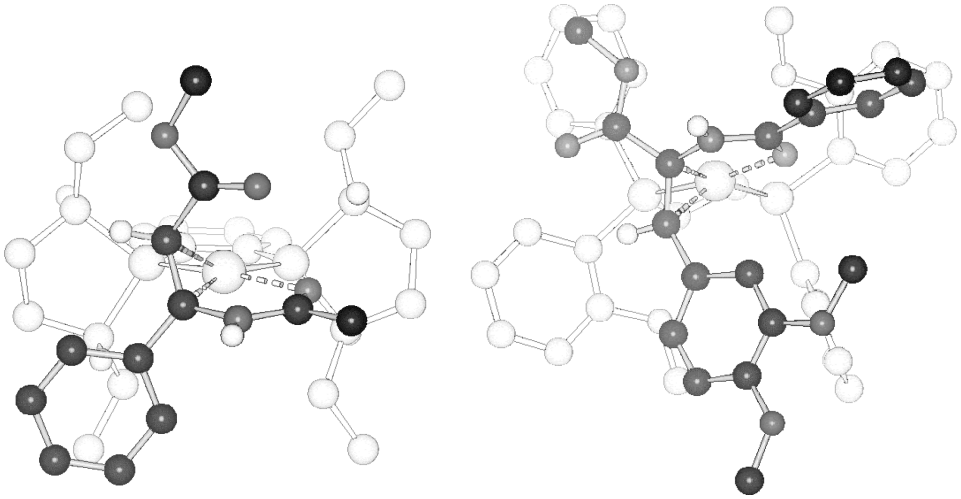

Fig. 10.23 X-ray structure of [Rh((*R*,*R*)-Et-DuPHOS)((*Z*)-3-*N*-acetylamino-3-(phenyl)-methyl propenoate)]$^+$ and of [Rh((*S*,*S*)-DIPAMP)((*Z*)-2-benzoylamino-3-(3,4-dimethoxyphenyl)-methyl acrylate)]$^+$ [62].

classical ideas [62a]. In these cases the major-substrate complex determines the selectivity, in analogy to the well known lock-and-key concept of enzyme catalysis proposed by Emil Fischer. This result could only be gained by quantitative monitoring of the hydrogenation and the subsequent interpretation of kinetic findings within the frame of Michaelis-Menten kinetics.

Abbreviations

COD	cycloocta-1,5-diene
NBD	norborna-2,5-diene
TOF	turnover frequency
TON	turnover number

References

1 R.A. Sanchez-Delgado, M. Rosales, *Coord. Chem. Rev.* **2000**, *196*, 249.

2 J.A. Widegren, R.G. Finke, *J. Mol. Cat. A: Chemical* **2003**, *198*, 317.

3 G. Djéga-Mariadassou, M. Boudart, *J. Catal.* **2003**, *216*, 89.

4 The number of reaction possibilities that fulfill particular limiting conditions can be surprisingly high. This is shown by mechanisms of various catalyzed reactions generated by computer programs such as ChemNet or MECHEM. (a) R.E. Valdes-Perez, A.V. Zeigarnik, *J. Chem. Inf. Comput. Sci.* **2000**, *40*, 833; (b) L.G. Bruk, S.N. Gorodskii, A.V. Zeigarnik, R.E. Valdes-Perez, O.N. Temkin, *J. Mol. Catal. A: Chem.* **1998**, *130*, 29; (c) A.V. Zeigarnik, R.E. Valdes-Perez, O.N. Tem-

kin, L.G. Bruk, S.I. Shalgunov, *Organometallics* **1997**, *16*, 3114.

5 According to Chen et al., alkali cation co-catalysis kinetics cannot be distinguished from classic ideas (proton instead of alkali) for the asymmetric hydrogenation of acetophenone with the Noyori-catalyst (*trans*-$RuCl_2$[(*S*)-BINAP][(*S*,*S*)DPEN]) (see [43b]).

6 J. Halpern, *Science* **1982**, *217*, 401.

7 R. Noyori, *Asymmetric catalysis in organic synthesis*. John Wiley & Sons, Inc., New York, **1994**.

8 W.A. Herrmann, B. Cornils, *Angew. Chem. Int. Ed.* **1997**, *36*, 1049.

9 (a) P.I. Dalko, L. Moisan, *Angew. Chem. Int. Ed.* **2004**, *43*, 5138; (b) Special edition *Accounts Chem. Res.* **2004**, *37*, 8, 487.

10 We point out that in enzyme kinetics TON is understood as TOF! "It is also sometimes called the turnover *number,* because it is a reciprocal time and defines the number of catalytic cycles (or "turnovers") that the enzyme can undergo in unit time, or the number of molecules of substrate that one molecule of enzyme can convert into products in one unit of time." Quotation from [23].

11 For the hydrogenation of acetophenone with the Ru-BINAP-DPEN system by Noyori, for example, in the course of 48 h 2.4 million conversions at the catalyst are reached (H. Doucet, T. Ohkuma, K. Murata, T. Yokozawa, M. Kozawa, E. Katayama, A.F. England, T. Ikariya, R. Noyori, *Angew. Chem. Int. Ed.* **1998**, *37*, 1703). Rautenstrauch could – under slightly changed conditions – reach a TOF of 333 000 h^{-1} (V. Rautenstrauch, X. Hoang-Cong, R. Churlaud, K. Abdur-Rashid, R.H. Morris, *Chem. Eur. J.* **2003**, *9*, 4954). The best results as concerns the activity of transfer hydrogenations were reported by Mathey, according to who cyclohexanone can, during the course of 15 h, be completely converted with a substrate/catalyst ratio of 20 million by a catalyst containing a P/N-ligand (C. Thoumazet, M. Melaimi, L. Ricard, F. Mathey, P. Le Floch, *Organometallics* **2003**, *22*, 1580).

12 The following TON and TOF specifications refer to minimum quantities for technically relevant processes: H.U. Blaser, B. Pugin, F. Spindler, *Enantioselective Synthesis, Applied Homogeneous Catalysis by Organometallic Complexes*, 2nd edn, Volume 3, B. Cornils, W.A. Herrmann (Eds.), Wiley-CH, Weinheim, **2002**, pp. 1131. "Catalyst productivity, given as substrate/catalyst ratio (*s/c*) or turnover number (TON), determines catalyst costs. These *s/c* ratios ought to be > 1000 for small-scale, high-value products and > 50 000 for large-scale or less-expensive products (catalyst re-use increases the productivity)" and "Catalyst activity, given as turnover frequency for > 95% conversion (TOF_{av}, h^{-1}), determines the production capacity. TOF_{av} ought to be > 500 h^{-1} for small-scale and > 10 000 h^{-1} for large-scale products" (p. 1133).

13 Due to *re-* and *si*-coordination of prochiral substrates at a catalyst with C_2-symmetric chiral ligands two diastereomeric catalyst-substrate complexes emerge. In the case of C_1-symmetric ligands already four stereoisomer intermediates result.

14 The so-called "minor-substrate complexes" of asymmetric hydrogenations are not detectable in many cases, even though they determine the stereochemical course of the hydrogenation due to their high reactivity according to classical ideas.

15 L. Michaelis, M.L. Menten, *Biochem. Z.* **1913**, *49*, 333.

16 M. Bodenstein, *Z. Phys. Chem.* **1913**, *85*, 329.

17 G.E. Briggs, J.B.S. Haldane, *Biochem. J.* **1925**, *19*, 338.

18 (a) F.G. Helfferich, *Kinetics of Homogeneous Multistep Reactions, Comprehensive Chemical Kinetics*, Volume 38, Elsevier, Amsterdam, **2001**; (b) K.A. Connors, *Chemical Kinetics. The Study of Reaction Rates in Solution*, VCH Publishers Inc., New York, **1990**.

19 "Quite often, kinetic studies are not performed because it appears time-consuming, expensive (with respect to the price or availability of most of chiral ligands) and not rewarding") (see [35a]).

20 An irreversible formation of the catalyst–substrate complex is described in: D.D.

van Slyke, G. E. Cullen, *J. Biol. Chem.* **1914**, *19*, 141.

21 (a) A. S. C. Chan, J. J. Pluth, J. Halpern, *J. Am. Chem. Soc.* **1980**, *102*, 5952; (b) C. R. Landis, J. Halpern, *J. Am. Chem. Soc.* **1987**, *109*, 1746; (c) M. Kitamura, M. Tsukamoto, Y. Bessho, M. Yoshimura, U. Kobs, M. Widhalm, R. Noyori, *J. Am. Chem. Soc.* **2002**, *124*, 6649.

22 Today, this synonym is used for the more common steady-state approach by Briggs and Haldane (see [17]).

23 A. Cornish-Bowden, *Fundamentals of Enzyme Kinetics*, 3rd edn, Portland Press Ltd., London, **2004**.

24 K. J. Laidler, *Can. J. Chem.* **1955**, *33*, 1614.

25 D. G. Blackmond, *Angew. Chem. Int. Ed.* **2005**, *44*, 4302.

26 At the end of a hydrogenation the substrate concentration is naturally also low.

27 The term for the saturation rate (V_{sat}) in earlier works commonly employed as "maximum rate" (V_{max}) should not – according to the recommendation of the International Union of Biochemistry – be used any more because it does not describe a real maximum, but a limit.

28 (a) A. G. Marongoni, *Enzyme Kinetics – A Modern Approach*, Wiley-Interscience, **2003**; (b) R. A. Copeland, *Enzymes – A Practical Introduction to Structure, Mechanism, and Data Analysis*, VCH Publishers, Inc., New York, **1996**; (c) H. Bisswanger, *Enzymkinetik*, VCH Verlagsgesellschaft mbH, Weinheim, **1994**; (d) A. Cornish-Bowden, *Principles of Enzyme Kinetics*, Butterworth & Co. Ltd., London, **1976**; (e) H.J. Fromm, *Initial Rate Enzyme Kinetics*, Springer, Berlin, **1975**; (f) I.H. Segel, *Enzyme kinetics*, Wiley & Sons, New York, **1975**.

29 H. Lineweaver, D. Burk, *J. Am. Chem. Soc.* **1934**, *56*, 658.

30 (a) G. S. Eady, *J. Biol. Chem.* **1942**, *146*, 85; (b) B. H. J. Hofstee, *J. Biol. Chem.* **1952**, *199*, 357; (c) B. H. J. Hofstee, *Nature* **1959**, *184*, 1296.

31 C. S. Hanes, *Biochem. J.* **1932**, *26*, 1406.

32 The original work of Lineweaver and Burk [29] is the most cited one in *J. Am. Chem. Soc.* (according to *Chem. Eng. News* **2003**, *81*, 27).

33 (a) Y. Fu, X.-X. Guo, S.-F. Zhu, A.-G. Hu, J.-H. Xie, Q.-L. Zhou, *J. Org. Chem.* **2004**, *69*, 4648; (b) H.-J. Drexler, J. You, S. Zhang, C. Fischer, W. Baumann, A. Spannenberg, D. Heller, *Org. Process Res. Dev.* **2003**, *7*, 355; (c) D. Heller, H.-J. Drexler, J. You, W. Baumann, K. Drauz, H.-P. Krimmer, A. Börner, *Chemistry – A European Journal* **2002**, *8*, 5196; (d) D. Heller, H.-J. Drexler, A. Spannenberg, B. Heller, J. You, W. Baumann, *Angew. Chem. Int. Ed.* **2002**, *41*, 777; (e) O. Pàmies, M. Diéguez, G. Net, A. Ruiz, C. Claver, *J. Org. Chem.* **2001**, *66*, 8364; (f) I. M. Angulo, E. Bouman, *J. Mol. Catal. A: Chemical* **2001**, *175*, 65; (g) N. Tanchoux, C. de Bellefon, *Eur. J. Inorg. Chem.* **2000**, 1495; (h) O. Pàmies, G. Net, A. Ruiz, C. Claver, *Eur. J. Inorg. Chem.* **2000**, 1287; (i) M. Rosales, A. González, M. Mora, N. Nader, J. Navarro, L. Sánchez, H. Soscín, *Trans. Met. Chem.* **2004**, *29*, 205; (j) C. A. Sandoval, T. Ohkuma, K. Muniz, R. Noyori, *J. Am. Chem. Soc.* **2003**, *125*, 13490; (k) A. Salvini, P. Frediani, S. Gallerini, *Appl. Organometal. Chem.* **2000**, *14*, 570; (l) V. Herrera, B. Munoz, V. Landaeta, N. Canudas, *J. Mol. Catal. A: Chemical* **2001**, *174*, 141; (m) P. K. Santra, P. Sagar, *J. Mol. Catal. A: Chemical* **2003**, *197*, 37; (n) M. Rosales, J. Castillo, A. González, L. González, K. Molina, J. Navarro, I. Pacheco, H. Pérez, *Trans. Met. Chem.* **2004**, *29*, 221; (o) M. Rosales, F. Arrieta, J. Castillo, A. Gonzàlez, J. Navarro, R. Vallejo, *Stud. Surf. Sci. Catal.* **2000**, *130*, 3357; (p) C. A. Thomas, R.J. Bonilla, Y. Huang, P.G. Jessop, *Can. J. Chem.* **2001**, *79*, 719.

34 A. Zogg, F. Stoessel, U. Fischer, K. Hungerbühler, *Thermochim. Acta* **2004**, *419*, 1.

35 (a) C. deBellefon, N. Pestre, T. Lamouille, P. Grenouillet, V. Hessel, *Adv. Synth. Catal.* **2003**, *345*, 190; (b) C. deBellefon, R. Abdallah, T. Lamouille, N. Pestre, S. Caravieilhes, P. Grenouillet, *Chimia* **2002**, 621; (c) J.L. Bars, T. Häußner, J. Lang, A. Pfaltz, D. G. Blackmond, *Adv. Synth. Catal.* **2001**, *343*, 207; (d) C. deBellefon, N. Tanchoux, S. Caravieilhes, P. Grenouillet, V. Hessel, *Angew. Chem. Int. Ed.* **2000**, *39*, 3442.

36 The real molar volume of hydrogen amounts to 24.48 cm^3 mol^{-1} at 25.0 °C and 1.013 bar (ideal gas: 24.46 cm^3 mol^{-1}). Due to non-linear compressibility, pV/p-isotherms at 100 bar deviate from ideal gas behavior by a few per cent.

37 Virial coefficients of hydrogen can, for example, be found in: J. H. Dymond, E. B. Smith, *The Virial Coefficients of Pure Gases and Mixtures*, Clarendon Press, Oxford, **1980**. By interpolation (e.g., with cubic spline functions), virial coefficients can be determined for any temperature.

38 B. Bogdanovic, B. Spliethhoff, *Chem.-Ing.-Tech.* **1983**, *55*, 156.

39 (a) Y. Sun, J. Wang, C. Le Blond, R.N. Landau, J. Laquidara, J. R. Sowa, Jr., D. G. Blackmond, *J. Mol. Catal. A: Chemical* **1997**, *115*, 495; (b) Y. Sun, R. N. Landau, J. Wang, C. LeBlond, D. G. Blackmond, *J. Am. Chem. Soc.* **1996**, *118*, 1348.

40 (a) J.-C. Charpentier, Mass-transfer rates in gas-liquid absorbers and reactors. In: *Advances in Chemical Engineering*, T. B. Drew, G. R. Cokeleit, J. W. Hoopes, Jr., T. Vermeulen (Eds.), Academic Press Inc., New York, **1981**, Volume 11, pp. 1; (b) G. Astarita, *Mass transfer with chemical reaction*, Elsevier Publishing Company, Amsterdam, **1967**.

41 Y. Sun, J. Wang, C. Le Blond, R. A. Reamer, J. Laquidara, J. R. Sowa, Jr., D. G. Blackmond, *J. Organomet. Chem.* **1997**, *548*, 65.

42 Such induction periods can, for example, result from transferring a precatalyst into the active species. For the asymmetric hydrogenation this is described in detail in: (a) W. Braun, A. Salzer, H.-J. Drexler, A. Spannenberg, D. Heller, *Dalton Trans.* **2003**, 1606; (b) H.-J. Drexler, W. Baumann, A. Spannenberg, C. Fischer, D. Heller, *J. Organomet. Chem.* **2001**, *621*, 89; (c) C. J. Cobley, I. C. Lennon, R. McCague, J. A. Ramsden, A. Zanotti-Gerosa, *Tetrahedron Lett.* **2001**, *42*, 7481; (d) A. Börner, D. Heller, *Tetrahedron Lett.* **2001**, *42*, 223; (e) W. Baumann, S. Mansel, D. Heller, S. Borns, *Magn. Res. Chem.* **1997**, *35*, 701; (f) D. Heller, S. Borns, W. Baumann, R. Selke, *Chem. Ber.* **1996**, *129*, 85.

43 (a) L. Greiner, M. B. Ternbach, *Adv. Synth. Catal.* **2004**, *346*, 1392 (supplementary information); (b) R. Hartmann, P. Chen, *Adv. Synth. Catal.* **2003**, *345*, 1353.

44 (a) A. G. Osborn, D. R. Douslin, *J. Chem. Eng. Data* **1974**, *19*, 114; (b) T. Boublik, K. Aim, *Collect. Czech. Chem. Comm.* **1972**, *11*, 3513; (c) D. W. Scott, *J. Chem. Thermodynamics* **1970**, *2*, 833; (d) T. E. Jordan, *Vapor pressure of Organic Compounds*, Interscience Publishers, Inc. New York, **1954**.

45 (a) P. G. T. Fogg, W. Gerrard, *Solubility of Gases in Liquids*, John Wiley & Sons, Chichester, **1991**; (b) E. Brunner, *J. Chem. Eng. Data* **1985**, *30*, 269.

46 To the best of our knowledge there are no experimental data available for CH_2Cl_2.

47 D. Heller, J. Holz, S. Borns, A. Spannenberg, R. Kempe, U. Schmidt, A. Börner, *Tetrahedron: Asymmetry* **1997**, *8*, 213.

48 (a) A. Aghmiz, A. Orejón, M. Dieguez, M. D. Miquel-Serrano, C. Claver, A. M. Masdeu-Bultó, D. Sinou, G. Laurenczy, *J. Mol. Catal. A: Chemical* **2003**, *195*, 113; (b) H. G. Niessen, P. Trautner, S. Wiemann, J. Bargon, K. Woelk, *Rev. Sci. Instrum.* **2002**, *73*, 1259; (c) S. Gaemers, H. Luyten, J. M. Ernsting, C. J. Elsevier, *Magn. Res. Chem.* **1999**, *37*, 25; (d) J. A. Iggo, D. Shirley, N. D. Tong, *New J. Chem.* **1998**, 1043; (e) A. Cusanelli, U. Frey, D. Marek, A. E. Merbach, *Spectr. Eur.* **1997**, *9*, 22; (f) S. Mansel, D. Thomas, C. Lefeber, D. Heller, R. Kempe, W. Baumann, U. Rosenthal, *Organometallics* **1997**, *16*, 2886; (g) W. Baumann, S. Mansel, D. Heller, S. Borns, *Magn. Reson. Chem.* **1997**, *35*, 701; (h) P. M. Kating, P. J. Krusic, D. C. Roe, B. E. Smart, *J. Am. Chem. Soc.* **1996**, *118*, 10000; (i) M. Haake, J. Natterer, J. Bargon, *J. Am. Chem. Soc.* **1996**, *118*, 8688; (j) K. Woelk, J. Bargon, *Rev. Sci. Instrum.* **1992**, *63*, 3307; (k) D. C. Roe, *J. Magn. Res.* **1985**, *63*, 388.

49 (a) L. Damoense, M. Datt, M. Green, C. Steenkamp, *Coord. Chem. Rev.* **2004**, *248*, 2393; (b) E. M. Vincente, P. S. Pregosin, D. Schott, *Mechanism in Homogeneous Catalysis – A Spectroscopic Approach*. B. Heaton (Ed.), Wiley-VCH,

2005, Chapter 1, pp. 1–80; (c) G. Laurenczy, L. Helm, *Mechanism in Homogeneous Catalysis – A Spectroscopic Approach*. B. Heaton (Ed.), Wiley-VCH, **2005**, Chapter 2, pp. 81.

50 D. Heller, W. Baumann, DE 102 02 173 C2, **2003**.

51 (a) D. Selent, W. Baumann, A. Börner, DE 10333143.A1 (3.3.**2005**); (b) D. Selent, W. Baumann, K.-D. Wiese, D. Ortmann, A. Börner, 14th International Symposium on Homogeneous Catalysis, Munich, 5.–9.7. **2004**, poster no. 0044.

52 Analogue trials in a cell are not practicable. To monitor hydrogen consumption accurately (ca. 8 mL in the example), an absolute quantity of COD is necessary. With equal catalyst/substrate ratios (as in the example), the resultant intracellular high catalyst concentration could only be compensated by a very small cell thickness, which would in turn considerably restrict intracellular mixing.

53 (a) S. Richards, M. Ropic, D. Blackmond, A. Walmsley, *Analytica Chim. Acta* **2004**, *519*, 1; (b) C. LeBlond, J. Wang, R. Larsen, C. Orella, Y.-K. Sun, *Topics Catal.* **1998**, 149; (c) C. LeBlond, J. Wang, R.D. Larsen, C.J. Orella, A.L. Forman, R.N. Landau, J. Laquidara, J.R. Sowa, D.G. Blackmond, Y.-K. Sun, *Thermochim. Acta* **1996**, *289*, 189.

54 A. Haynes, *Mechanism in Homogeneous Catalysis – A Spectroscopic Approach*. B. Heaton (Ed.), Wiley-VCH, **2005**, Chapter 3, pp. 107.

55 (a) J.M. Brown, P.A. Chaloner, *J. Chem. Soc., Chem. Commun.* **1980**, 344; (b) J.M. Brown, P.A. Chaloner, *Homogeneous Catalysis with Metal Phosphine Complexes*. L.H. Pignolet (Ed.), Plenum Press, New York, **1983**, pp. 137; (c) J.M. Brown, *Chem. Soc. Rev.* **1993**, *22*, 25.

56 A review regarding experimental findings, which seemingly speak for the alternatively discussed dihydride mechanism, can be found in: I.D. Gridnev, T. Imamoto, *Acc. Chem. Res.* **2004**, *37*, 633. However, it must be stressed that verified results such as the pressure dependence of enantioselectivity cannot be described by this model. Models related to the dihydride mechanism and developed substantially on the basis of low-temperature NMR spectroscopy have not yet been investigated in terms of kinetic consequences.

57 (a) J.M. Brown, P.A. Chaloner, G.A. Morris, *J. Chem. Soc., Chem. Commun.* **1983**, 664; (b) J.M. Brown, P.A. Chaloner, G.A. Morris, *J. Chem. Soc., Perkin Trans. II* **1987**, 1583; (c) H. Bircher, B.R. Bender, W. von Philipsborn, *Magn. Reson. Chem.* **1993**, *31*, 293; (d) R. Kadyrov, T. Freier, D. Heller, M. Michalik, R. Selke, *J. Chem. Soc., Chem. Commun.* **1995**, 1745; (e) J.A. Ramsden, T.D.W. Claridge, J.M. Brown, *J. Chem. Soc., Chem. Commun.* **1995**, 2469; (f) D. Heller, R. Kadyrov, M. Michalik, T. Freier, U. Schmidt, H.W. Krause, *Tetrahedron: Asymmetry* **1996**, *7*, 3025; (g) A. Kless, A. Börner, D. Heller, R. Selke, *Organometallics* **1997**, *16*, 2096.

58 In case of the asymmetric hydrogenation with Rh complexes this disturbance in the equilibrium establishment is shown in pressure-dependent e.e. values (see [21b]). Djega-Mariadassou and Boudart [3] describe this phenomenon as "kinetic coupling"; see also G. Djega-Mariadassou, *Catal. Lett.* **1994**, 7. In this context, we point out that under "kinetic coupling" conditions it is principally not possible experimentally to determine a partial order of 1 with respect to hydrogen.

59 D. Heller, R. Thede, D. Haberland, *J. Mol. Cat. A: Chemical* **1997**, *115*, 273.

60 This statement also applies if intermolecular pre-equilibria are not established. In case of established intermolecular pre-equilibria the value of $1/K_M$ corresponds to the sum of all stability constants.

61 (a) H.W. Krause, H. Foken, H. Pracejus, *New J. Chem.* **1989**, *13*, 615; (b) H.W. Krause, U. Schmidt, S. Taudien, B. Costisella, M. Michalik, *J. Mol. Catal. A: Chemical* **1995**, *104*, 147; (c) C. Döbler, H.-J. Kreuzfeld, M. Michalik, H.W. Krause, *Tetrahedron: Asymmetry* **1996**, *7*, 117; (d) H.J. Kreuzfeld, C. Döbler, U. Schmidt, H.W. Krause, *Amino Acids* **1996**, *11*, 269; (e) U. Schmidt, H.W. Krause, G. Oehme, M. Michalik, C. Fischer, *Chirality* **1998**, *10*, 564;

(f) C. Döbler, H.-J. Kreuzfeld, C. Fischer, M. Michalik, *Amino Acids* **1999**, *16*, 391; (g) T. Dwars, U. Schmidt, C. Fischer, I. Grassert, H.W. Krause, M. Michallik, G. Oehme, *Phosphorus, Sulfur, and Silicon* **2000**, *158*, 209.

62 (a) H.-J. Drexler, W. Baumann, T. Schmidt, S. Zhang, A. Sun, A. Spannenberg, C. Fischer, H. Buschmann, D. Heller, *Angew. Chem. Int. Ed.* **2005**, *44*, 1184; (b) H.-J. Drexler, S. Zhang, A. Sun, A. Spannenberg, A. Arrieta, A. Preetz, D. Heller, *Tetrahedron: Asymmetry* **2004**, *15*, 2139.

63 T. Schmidt, W. Baumann, H.-J. Drexler, A. Arrieta, D. Heller, H. Buschmann, *Organometallics* **2005**, *24*, 3842.